City Research Online

City, University of London Institutional Repository

Citation: Qassem, M. & Kyriacou, P. A. (2019). Review of Modern Techniques for the Assessment of Skin Hydration. Cosmetics, 6(1), 3. doi: 10.3390/cosmetics6010019

This is the published version of the paper.

This version of the publication may differ from the final published version.

Permanent repository link: https://openaccess.city.ac.uk/id/eprint/21851/

Link to published version: https://doi.org/10.3390/cosmetics6010019

Copyright: City Research Online aims to make research outputs of City, University of London available to a wider audience. Copyright and Moral Rights remain with the author(s) and/or copyright holders. URLs from City Research Online may be freely distributed and linked to.

Reuse: Copies of full items can be used for personal research or study, educational, or not-for-profit purposes without prior permission or charge. Provided that the authors, title and full bibliographic details are credited, a hyperlink and/or URL is given for the original metadata page and the content is not changed in any way.

City Research Online: http://openaccess.city.ac.uk/ publications@city.ac.uk

cosmetics

MDPI

Article

Review of Modern Techniques for the Assessment of Skin Hydration

Meha Qassem *,† **and Panayiotis Kyriacou** †

Research Centre for Biomedical Engineering (RCBE), City, University of London, Northampton square, London EC1V 0HB, UK; p.kyriacou@city.ac.uk

* Correspondence: meha.qassem.1@city.ac.uk; Tel.: +44-7040-3878

† These authors contributed equally to this work.

Received: 11 February 2019; Accepted: 6 March 2019; Published: 9 March 2019

Abstract: Skin hydration is a complex process that influences the physical and mechanical properties of skin. Various technologies have emerged over the years to assess this parameter, with the current standard being electrical probe-based instruments. Nevertheless, their inability to provide detailed information has prompted the use of sophisticated spectroscopic and imaging methodologies, which are capable of in-depth skin analysis that includes structural and composition details. Modern imaging and spectroscopic techniques have transformed skin research in the dermatological and cosmetics disciplines, and are now commonly employed in conjunction with traditional methods for comprehensive assessment of both healthy and pathological skin. This article reviews current techniques employed in measuring skin hydration, and gives an account on their principle of operation and applications in skin-related research.

Keywords: skin hydration; barrier function; stratum corneum

1. Introduction

The skin is the interface between humans and their environment. It acts as a means of adjusting to variations in environmental temperatures through elegant controls that regulate microcirculation, and as an impermeable barrier that allows the body to intake water without flooding its internal organs, all while prohibiting the intrusion of various xenobiotics. The outermost layer of the skin, known as the stratum corneum (SC), consists of piled-up layers of flattened corneocytes separated by lipids in the intercellular space. Together, they serve as the primary skin barrier. The skin's functions and dysfunctions, which include many pathological conditions, have huge impact on both the physical health and self-esteem of a person [1,2].

Over the years, numerous studies have contributed to understanding the skin, and provided many tools for treatment and diagnostic purposes. An absolute interdisciplinary approach has been taken to envelop many disciplines such as analytical sciences, instrumentation, and traditional dermatological and cosmetic sciences, the latter playing a major role in assessing the ingredients of personal care products and evaluating their functional efficacy.

Such advancements have greatly extended our understanding of the structural arrangement and functional characteristics of skin, and led to the development of various instruments that can be used for this purpose. Since previous interpretations of dry skin assumed a lack of water in the SC, earlier methods and devices were focused on determining the water content of the SC, while more recent techniques such as Raman analysers and infrared spectrometers, have aimed at addressing not only the water content, but also other skin constituents such as lipids and proteins, and their overall relationship with skin hydration.

This paper reviews current techniques used for the assessment of skin hydration, including traditional probe-based devices as well as spectroscopic and imaging modalities. Several techniques are correlated with the gold standard skin capacitance method, and hence correlations and comparisons are also briefly discussed within.

2. Differential Scanning Calorimetry

Differential Scanning Calorimetry (DSC) is a thermal technique used to determine the energy of thermal transitions, and permits quantification of their temperature dependence. Initially developed in the early 1960s, DSC remains the reference method for characterising bound, bulk and free water molecule types inside the SC because it can directly measure the energies of interactions and phase changes of multiple SC composites [3,4].

DSC instrumentation operate using heat flux or power compensation methods, both of which measure the heat in or out of a sample relative to a reference. A sample of SC layer is usually studied relative to a reference of distilled water, giving an output DSC thermogram that shows the instant power provided or the absorbed power related to the transition phenomenon observed. Calculating the area under each peak gives the enthalpy of the coinciding transition.

A typical thermogram of the SC is composed of several peaks. The first peak is not always apparent and can disappear if an organic solvent is added to the SC sample due to the melting of sebaceous lipids on the skin surface [4,5]. The second peak is assumed to reflect the melting of hydrophobic chains present in the lipid bilayers and the third, although difficult to interpret, has been suggested to relate to the changes imposed by heat in the lipid-protein complex between the intercellular lipids and corneocyte membrane [4–6]. Moreover, this peak is highly sensitive to hydration, and when the SC water content increases, its transition temperature and area are reduced [5,7]. The fourth and final peak is thought to be linked to thermal denaturation of intracellular keratin, which is irreversible and is also seen in lipid-free SCs [4,5,7–9].

Al-Saidan et al. [10] investigated the thermal transitions in desiccated SC membranes of adult abdominal human skin and concluded that extraction of SC using solvents decreased the content of bound water, whereas extraction by water maintained the same content.

Although earlier studies using DSC were focused on studying the mechanical or biophysical properties of skin and its basic composition [11–14], the technique remains popular and continues to be employed in studies of cosmetic ingredients [15–18] and liposome-assisted drug delivery [19–24], where DSC serves as a primary tool in characterizing the matrix state, with polymorphism and drug incorporation in lipid dispersions [3].

3. Electrical-Based Methods

The skin possesses electrical properties that relate to SC hydration through various types of electroconductivity elements, with protonic conduction being the predominant type in electrical measurements of skin hydration. Electrical-based methods consider a simple electrical model of the skin as a resistor connected in parallel with a capacitor, which together, contribute to the total skin impedance, $\boldsymbol{Z}$. When an alternating current of frequency, f, is applied to the skin, the value of $\boldsymbol{Z}$ will depend on the contribution of the resistance, $\boldsymbol{R}$, and capacitance, $\boldsymbol{C}$: $Z = (R^2 + 1/2\pi fC^2)^{\frac{1}{2}}$. By using measuring electrodes of adequate geometry, and a suitable applied frequency and design of oscillating electronic circuit, electrical-based devices can determine either the capacitance, conductance, or impedance contributions related to skin hydration.

Skin capacitance and conductance: This principle is based on the classical operation of a capacitor, whose main role is to store electrical charge when it comes close to a charged field, and is comprised of at least two electrical conductors separated by an insulating material acting as a dielectric [25]. The dielectric constant of water differs from other substances, and is 81 compared to roughly <7 from most others. Thus, water is much more powerful at enhancing the capacity of a

capacitor, and this leads to the assumption that skin capacitance is directly proportional to skin water content, and the higher the hydration level in the SC, the higher the capacitance [25].

The skin capacitance method is widespread and has become the standard measure of skin moisture, especially with a handheld device known as the Corneometer® (Courage & Khazaka, Cologne, Germany). Since its development in 1980, the Corneometer® has been used in numerous cosmetics and dermatological studies, either on its own or in conjunction with other devices, and is still used in correlation studies of comparable methods. The MoistureMeter(Delphin Technologies Ltd., Kuopio, Finland) is another commercial device based on capacitance measurements.

Skin conductance is an alternative approach for measurement of skin moisture derived from alterations in the electrical properties of the SC. A layer of SC with high water content produces stronger and more sensitive electrical conductivity than dehydrated SC, and increases the induction of the dielectric constant [25]. Generally, this gives larger conductance and capacitance values but reduces the impedance value of skin. A popular device implementing this method is the Skicon® (IBS Co., Hamamatsu, Japan), which is often preferred because it overcomes the issue of false or inaccurate readings experienced by capacitance and impedance measurements due to external influences. The Skicon® can reduce these influences by applying a higher frequency of 3.5 MHz on closely spaced electrodes inside a probe that maintains the electric field within the superficial layers of skin [25].

More recently, a new technique based on image micro-sensing has been developed, which performs in vivo mapping of skin surface capacitance and provides a non-optical image of SC moisture [26]. The first device, known as the SkinChip® was developed by L'Oreal, with others such as the MoistureMap (Courage & Khazaka, Cologne, Germany) soon following. A typical sensor of this kind is composed of an array of micro-capacitors distributed on a thin silicon oxide plate that produces grey level images once applied onto the skin with sustainable pressure at a level of every 50 µm [27,28]. Further analysis of the image via computer software gives the average grey level of the image histogram, which can then be used to obtain the average capacitance of skin surface (Figure 1). Comparative studies between the SkinChip® and Corneometer® showed a good correlation between the two devices, and deemed it a necessary tool for complete analysis and quantification of skin surface hydration [27,29].

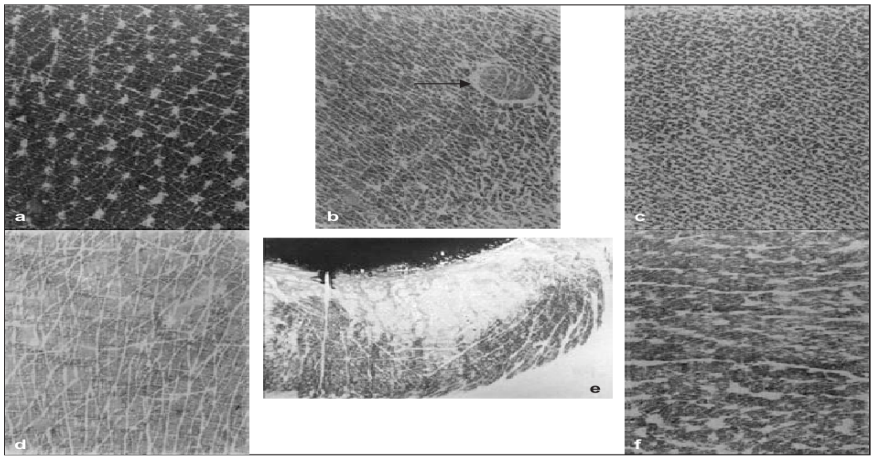

Figure 1. Capacitance imageing of skin surface at six anatomical sites. (**a**) Lateral side of the neck, (**b**) Abdomen. The arrow points to a ruby angioma appearing as a circumscribed lesion with an altered pattern of skin linenetwork. (**c**) Inner aspect of the arm with a very dense network of microrelief lines. (**d**) Dorsum of the hand, (**e**) Lower lip, (**f**) Forehead [29].

The combination of skin surface imaging and detailed analytical quantification of corneocyte hydration provided by capacitance imaging has created new research opportunities in investigating SC hydration [30–32], sweat gland activity [33–35], skin microrelief and ageing [36,37], and the effects

of topical applications [38–40]. The technique has also been used for diagnostic purposes or general examinations of skin physiology [26,27]. Furthermore, skin capacitance mapping has recently been incorporated into the revised EEMCO guidelines for in vivo measurement of skin water [41].

Skin impedance: Opposite to capacitance and conductance, skin impedance evaluates the resistance of skin, which increases with dehydration of the SC layer and is influenced by the composition and metabolic activity of skin. Commercial products implementing this principle include the Nova® Dermal Phase Meter (Nova, Waltham, MA, USA) and the Surface-Characterizing Impedance monitor (SCIM) (U.S. Pat. No. 5353802, issued 11 October 1994). These instruments integrate the readings taken at separate frequencies of the applied alternating current, and generate impedance-based capacitance values. Unlike the Corneometer® and Skicon®, which use a low frequency range or a fixed frequency, the Nova® Dermal Phase Meter measures samples along a controlled rise time of up to 1 MHz. The Surface-Characterizing Impedance monitor is also capable of magnitude and phase outputs.

4. Transepidermal Water Loss

Transepidermal Water Loss (TEWL) is characterised by the constitutive evaporation of water that initiates from the deeper, more hydrated layers of the epidermis and dermis and then moves towards the more superficial SC layer, in the absence of sweat gland activity. Depending on climate conditions, a portion of this water evaporates through the SC whilst some is preserved within by the presence of NMFs, which in turn, directly relate to skin hydration and barrier function. If the integrity of SC barrier function is compromised, more water can escape, and TEWL increases. Nevertheless, elevated levels of TEWL is not an indication of SC damage, particularly when is accompanied by alterations in temperature and hydration, but it is a very valuable and commonly used tool in dermato-cosmetic tests, particularly when examining the effects of various products and conditions on SC barrier function.

TEWL can be measured through four different mechanisms:

Open chamber: This mechanism follows the basic theory of Fick's law of diffusion, and is the traditional method for TEWL measurements. The set-up consists of a chamber made up of two pairs of temperature and humidity sensors, placed inside a hollow cylinder. The overall system estimates the water gradient through the open chamber and allows continuous readings of ambient air, with little variation in the microclimate overlying the skin surface. Commercially available instruments include the Tewameter® (Courage & Khazaka, Cologne, Germany), DermaLab® (Cortex Technology ApS, Hadsund, Denmark) and the Evaporimeter® (ServoMed, Varberg, Sweden). When using these, it is essential to maintain a controlled environment as many factors such as probe size, airflows from atmosphere and the body, room temperature, air convection, and ambient humidity can easily alter results [42,43].

Closed chamber: This system is composed of humidity and temperature sensors placed in a closed cylindrical chamber. Upon application on the skin, the relative humidity (RH %) increases and is used to detect the rate of TEWL [44,45]. A popular device of this type is the VapoMeter® (Delfin Technologies Ltd., Kuopio, Finland), which has proved through comparative studies [45,46] to give more accurate and rapid readings. Unlike open chamber instruments, the closed chamber system of the VapoMeter® is not affected by ambient or body-induced airflows but its rapid assessment makes it susceptible to interference from movements, surface moisture and tremor, and is unable to perform continuous measurements because it uses the principle of single point readings [42].

Ventilated closed chamber: This approach follows the flow principle, and measures the humidity of ambient air flowing into a closed chamber. The closed chamber is placed onto the skin surface with air passing through it, which causes TEWL to be removed. Air humidity is calculated before it is released back into the surrounding, and thus, the rate of TEWL is determined by estimating the difference in humidity before and after contact with skin [45]. The set-up allows continuous recording of TEWL rates, but can be unreliable if the carrier gas is too dry because it will artificially enhance evaporation [25].

Condenser chamber: This is a more recent method whereby a closed chamber contains a cold plate that condenses moisture into ice using a Peltier system. The system eliminates accumulation of moisture by removing it from the chamber, a problem that normally occurs in unventilated chambers [45]. The Biox Aquaflux® (Biox Systems Ltd., London, UK) is an example of this technique, which uses diffusion gradient to give TEWL readings. Its probe is designed with a closed top, achieved by a condenser that is constantly removing water vapour from air in its vicinity by freezing [47]. It has two sensors; one positioned halfway of the chamber and the other inside the condenser. Replacement caps are available for measurements on several body sites [47]. Again, comparative studies on this method have shown its data to correlate well with alternative instruments, even under several climate conditions and geometric dimensions [47–49].

Measurements of TEWL are often employed in regulatory testing, and to claim support for cosmetic products [50]. Some claim-support parameters for which TEWL readings have been used include reduction of irritating skin reactions, skin mildness, modulation of SC barrier function, increase in skin hydration, and protection against sun damage. Moreover, TEWL measurements are used in aiding the development of novel cosmetic ingredients, and products designed to repair SLS damage [51,52], or for atopic/eczematic [53,54] and aged skin [55–59]. Additional applications include improving topical therapeutic treatments, and as a non-invasive tool in skin compatibility testing of cosmetic products on human skin.

5. Skin Elasticity

Skin elasticity relates to the elastic properties of skin and its flexibility. It is determined through measurement of tensile, rheological, and biochemical parameters under mechanical stress. Assessment of skin elasticity is important in both cosmetics and dermatology because it is believed to decrease with chronological and photo- ageing, and has experimentally proved to rise with hydration levels.

Measurements of skin elasticity are typically performed using non-invasive techniques, of which two methodologies exist that apply skin deformation either in the plane of the skin e.g., torsion, or horizontally to it e.g., suction or indentation. In this case, measured parameters are obtained indirectly and can reveal complex skin attributes including the arrangement of dermal collagen and elastic fibres, and the desquamation process. Therefore, it is difficult to solely rely on mechanical methods for hydration measurements and additional techniques are often incorporated into this assessment.

Methods using deformation in the plane of the skin tend to focus more on the properties of superficial tissues, which give information regarding geometric dimensions and require smaller deformations. This includes the torsion technique, which evaluates the skin's resistance to torsion as applied by a rotating disc, and it is beneficial when trying to lessen the effects of dermis-hypodermis interrelations [60]. Initially, torsion-based systems lacked ability to restrict the geometry of the measurement zone but following vast improvements, commercial devices such as the Dermal Torque Meter® and Twistometer® (Both from Dia-Stron, Hampshire, UK) became available. The operating principle involves induction of a given amount of stress using a rotating disc adhered to the skin, and then measuring the angular displacement of the resulting skin deformation. A concentric guard ring, also adhered to the skin, limits the size of the area subject to stress. Using the geometry and a few simplifying approximations, the Young's modulus i.e., stiffness measure of an elastic material, can be determined.

An experiment carried out by De Rigal and Leveque [61] showed that for a distance of 1 mm and coupling of 0.6 N m, the dermis was undeformed, and only the epidermis and SC were deformed. Thus, for a given torsion couple, an increase in the distance between the central disc and the guard ring deepens the deformation of skin during torsion [61].

The torsion method has been widely used to assess moisturiser formulations and their hydrating efficacy [62–64], as well as complementing capacitance/conductance measurements [65] in evaluating performance claims of skin care ingredients, an alliance that continues to be implemented today.

Outside of cosmetic applications, racial and gender differences have been examined in relation to skin structure and function [66–68], and in studies of skin ageing [69–73] investigating changes in mechanical properties, particularly the elastic return feature, and the effects of sun exposure and photodamage. A successful implementation of this technique is the creation of the "skin condition chart" by Salter et al. [70], which is based on the torsional mechanical characteristics of skin, assessed using the Dermal Torque Meter®.

As for techniques applying deformation horizontal to the skin, suction is most commonly selected in commercial devices such as the Cutometer® (Courage & Khazaka, Cologne, Germany) and the DermaFlex® (Cortex Technology, Hadsund, Denmark), with the former considered the standard instrument in dermatology and cosmetology for the measurement of skin elasticity. These are merely suction devices that work by inducing a vacuum suction perpendicular to the skin surface, and then determine the resulting displacement and relaxation of skin. Data is expressed by the same standardised parameters regardless of whether the force is applied horizontally or in parallel to the plane of skin. Skin thickness has strong influence on the measured parameters, and in turn, is dependent on the geometry and size of the probes exercised. Therefore, measurements must be carried out under controlled settings and many factors including pressure, vacuum load, position, time of application and relaxation, and pretension of the skin must remain constant throughout the examination period [60,74].

The Cutometer® can yield reasonably accurate and reproducible stress-strain and strain-time curves that can emphasis the pure elasticity and viscoelasticity of the dermis [74]. Evaluating the SC alone is difficult, and thus elasticity data is normally presented as a ratio e.g., U_r/U_f, known as the biologic elasticity. Alternatively, The DermaFlex® employs a proportional full-thickness strain method rather than the disproportional superficial strain system used by the Cutometer®. This method is regularly employed in studies of skin pathology and scars [75–83], environmental and natural effects on skin [84–88], as well as anti-ageing cosmetic preparations [89–94]. Quite often, the DermaFlex® is used for dermatologic purposes whereas the Cutometer® is more commonly used in cosmetic studies [60,74].

6. Photothermal Radiometry

Photothermal radiometry, also termed Opto-Thermal Transient Emission Radiometry (OTTER), is a non-invasive, non-occlusive method, which uses excitation and thermal emission wavelengths that are strongly absorbed by the top few microns of the SC and are specific to the spectral properties of water [95]. Excitation and radiation from deeper layers of the skin do not affect measurements due to the low thermal diffusivity of skin, and the effects of optical scattering are also negligible because of the dominance of absorption and the low turbidity of skin at the long wavelengths used [95]. Together, this gives results that resemble a semi-infinite homogeneous material. In principle, the excitation wavelength (α) is greater than the wavelength of emitted thermal radiation (β), and so the resulting excitation is in photothermal saturation, and the signal $S(t)$ can be described by:

$$S(t) = Ae^{\frac{t}{\tau}} erfc(\sqrt{t/\tau} \quad (1)$$

with A being a constant, τ, the opto-thermal decay time (defined as $\tau = \frac{1}{\beta^2 D}$), and D, the thermal diffusivity.

Subsequently, a single parameter, τ, can be used to determine skin hydration, and can be obtained in vivo as it is insensitive to experimental variables such as optical alignment and amounts of absorbed energy. Moreover, the opto-thermal decay time (τ) relates to two fundamental parameters, β and D, thereby permitting absolute calibration of the instrument once their dependence on hydration is found [95].

Initial experimentation was introduced by Imhof et al. [96,97] followed by Xiao et al. [98], and has been applied in a range of skin measurements including SC water content [99–102], pigmentation (particularly port wine stains) [103–105], nails [106], solvent penetration [107,108],

and computational modelling of skin [109–111]. A study on the water-keratin interaction in relation to free and bound water in the SC [99] correlated OTTER results with previous findings from Leveque et al. [112], showing that the absorption band of bound water at low humidity shifted towards high wavelengths, and was narrower than the band associated with bulk water. A downward shift of 30 nm was observed when the relative humidity increased from 3% to 100%, and showed a plateau between 10% and 40% RH on delipidized samples. For normal SC, the decay was normal.

Further studies on SC hydration include measurement of epidermal thickness [113], SC renewal time [114] and SC water concentration gradient [100–102]. These concluded that OTTER is capable of measuring water content at the skin surface as well as water concentration gradient within the SC, water status in the SC, SC thickness, and SC swelling during hydration. Moreover, combining the OTTER with TEWL allowed determination of SC water-holding capabilities (Figure 2). Recent efforts in combining OTTER with infrared spectroscopy [115,116] or even 2D detection promises photothermal spectroscopy/photothermal microscopy that is depth resolved and could simultaneously obtain spectral information from the skin surface and deeper layers.

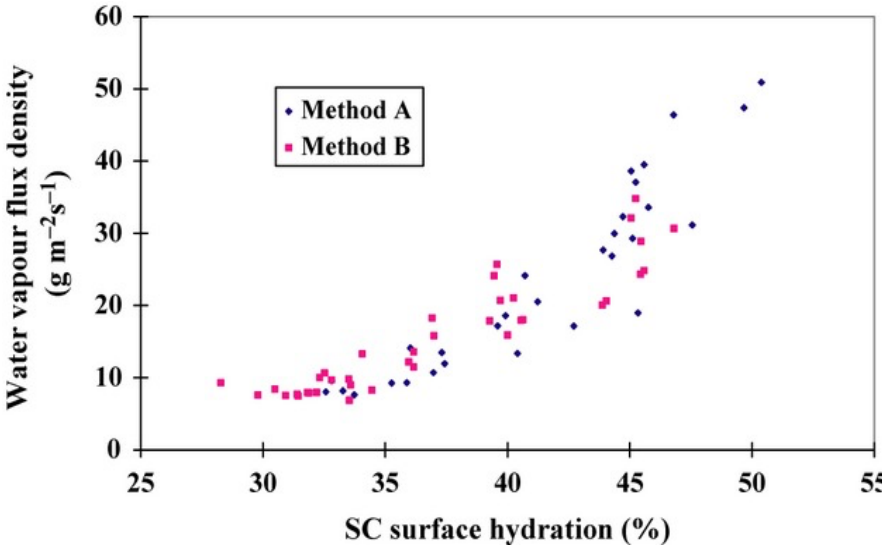

Figure 2. Water vapour flux density (WVFD) data (Method A) versus opto-thermal transient emission radiometry (OTTER) (Method B) from the volar forearm [102].

7. Attenuated Total Reflection Infrared Spectroscopy

Attenuated Total Reflection Infrared (ATR-IR or ATR-FTIR) spectroscopy is based on the attenuation of the evanescent wave generated by totally reflected IR radiation on an internal reflectance element (IRE) crystal. Every time a reflection occurs by the surface of the attached crystal, the skin absorbs part of the energy due to the evanescent wave theory and the electromagnetic nature of light. The amount of energy absorbed by the skin is recorded on a spectrum by a suitable infrared detector, and has the advantage of only analysing the first micron of the SC due to the submicronic penetration of evanescent waves.

For skin hydration measurements, a beam of polychromatic IR light is shone on the skin surface, and depending on the type of crystal used, several reflections are produced between the upper surface of the crystal and that of the skin before light is returned to the spectrometer. Every time a reflection occurs on the skin, the beam penetrates a small distance into the SC, where it is absorbed. The generated IR spectrum shows the IR absorption bands of the SC.

Various approaches have been reported for measuring SC water content using this technique, including calculating the ratio between the amide I and amide II bands at 6.06 and 6.45 µm, or between the absorbance at 1.95 and 1.8 µm, or by measuring the absorbance at 8.94 µm and 9.65 µm and then calculating the area of the water absorbance peak at 4.76 µm. Nevertheless, measurements may require

calibration with standards, and absorption intensities are susceptible to influences from the presence of moisturisers or other products on the skin surface. As mentioned earlier, results are also limited to superficial SC layers due to weak IR beam penetrations, which are only capable of reaching a depth of 5–20 µm.

An early study by Potts et al. [117] used this technique to quantitatively determine the water content in the SC through a combination of in vivo and in vitro examinations, and again later by Bommannan [118] to assess the SC barrier function in vivo. Boncheva et al. [119] used second derivative IR spectra for evaluation of lateral lipid chain packing, and was able to detect the presence and extent of OR and HEX phases. The report suggested that ATR-FTIR can be used for both in vivo and ex vivo assessments of SC barrier function and lateral lipid organisation changes resulting from topical application of products, and to provide information on the molecular basis of interactions. It has also been possible to study lipid molecular organisation in relation to SC integrity and cohesion in healthy human skin [120] using ATR-FTIR, as well as lipid-lamellae phase behaviours in the axilla, which showed reduced barrier function in this anatomical region [121]. At present, the technique is commonly combined with additional modalities such as Raman Spectroscopy for evaluation of molecular organisation of SC lipids and corneocytes in drug penetration [122–126] and detection of unwanted drug crystallisation within skin [127], as well as in cosmetic studies of the distribution of phospholipids-based formulations [128] and moisturiser penetration [129,130].

The main limitation of ATR-IR/FTIR stems from the pressure required to obtain a good signal-to-noise ratio, which can cause occlusion and accumulation of water at the test site. Furthermore, the water band at 1640 cm^{-1} exhibits a frequency that coincides with the protein amide I vibration at 1645 cm^{-1}, and is thus susceptible to variations from moisture levels. Although Potts et al. [96] substituted this band with 2100 cm^{-1}, which had the betterment of being in the mid-IR region and away from protein or formulation ingredients peaks, it is very weak and sometimes inconspicuous in dry skin [131].

8. Nuclear Magnetic Resonance

Nuclear Magnetic Resonance (NMR) takes advantage of the magnetic properties of the nucleus to sense the proximity of electronegative atoms, double bonds, and other magnetic nuclei nearby in the molecular structure. In practice, NMR measurements are acquired by placing a sample in an intense magnetic field, causing a nuclear spin that is aligned with the field axis. Radiofrequency waves are then used to excite the nuclei, resulting in vibrations or resonance perpendicular to the field axis. At the end of the excitation process, the induced spin begins to relax and finally returns to a state of equilibrium. This relaxation creates the NMR signal, which is then used to specify the atoms and molecules of the sample in question. The final NMR signal can be portrayed as a spectrum of resonance by magnetic resonance spectroscopy or as an image, using Magnetic Resonance Imaging (MRI).

A study by Hasen and Yellin [132] combined NMR and IR modalities to investigate the state of water in a variety of in vitro human SC. NMR served as a direct measure of molecular mobility whereas IR spectroscopy was used to provide information on the strength of inter-molecular hydrogen bonding. Their results confirmed the existence of three species of water in hydrated SC, but unlike IR spectra, NMR time-scale spectra were only able to distinguish bulk liquid-like water. Many studies afterwards focused on measurement of free and bound water [133] or on the relationship between water and non-aqueous skin components i.e., lipids and proteins within healthy SC [134,135], and even that affected by psoriasis [136]. A more recent study by Silva et al. [137] carried out a detailed assessment of the hydration process in extracted SC lipids, isolated corneocytes and intact SC using micro-calorimetry and NMR. Some of the findings were later confirmed by Bjorklund et al. [138] who found that heating had a strong effect on lipid mobility, and hydration in excess of 85% RH caused abrupt changes to keratin filament dynamics. Moreover, the structure of anti-ageing and moisturiser ingredients are commonly investigated using NMR prior to formulation [139–141], and in investigations of molecular mobility of SC barrier function [142,143].

As for MRI images, each point within an image is pertained to a particular signal intensity caused by a given small volume of tissue. Compared to alternative imaging modalities, MRI has proved advantageous in assessing skin water content and other parameters due to its ability to provide tissue imaging as well as physical-chemical classification, where alternatives such as radiography and ultrasound only give information pertaining to tissue density and mechanical interface differences, respectively. Unfortunately, an MRI device suitable for skin measurements is not available, which would require a minimum resolution of 100 µm due to variations in skin thickness [60].

Nevertheless, an imaging probe connected to a standard whole-body imager at 1.5 Tesla was attempted by Bittoun et al. [144], who then used the accessory to record in vivo images of multiple anatomical sites at an axial resolution of 70 µm. The images produced were able to differentiate the epidermis, dermis, and hypodermis from various anatomical sites, and were then used to evaluate skin hydration in young and old individuals using proton density data that correspond to the content of unbound or free water [145].

Franconi et al. [146] reported an alternative approach to measuring skin hydration by using the BIOSPEC® imager (Bruker Optik GmbH, Ettlingen, Germany). When combined with a specific probe and image acquisition sequence, the device produces images of forearm skin with an axial resolution of 86 µm. The study measured the relaxation time (T2) at the epidermal level and showed an increase after use of hydrating creams. As this function is wedded to the content of free water, its increase signified betterment in epidermal hydration. Furthermore, the moisturising effect of cosmetic products was investigated by Szayna and Kuhn [147] using high-field MRI and NMR microscopy, and then later by Mesrar et al. [148] who examined MRI images acquired in vivo prior to and after moisturiser application, and reported a T2 increase in both SC and epidermis without significant difference in the dermis layer (Figure 3).

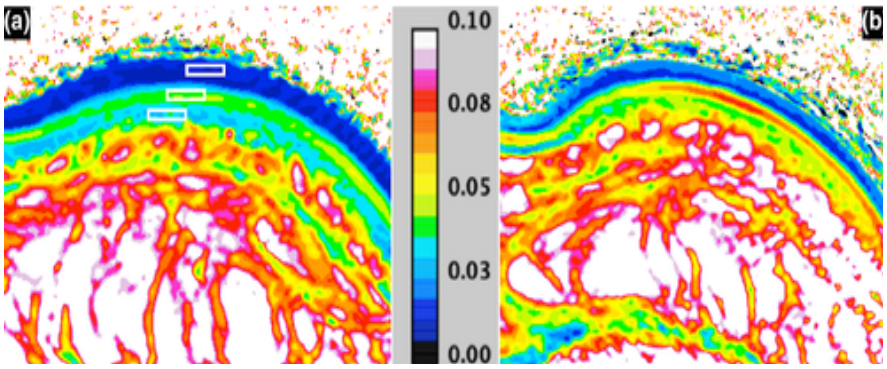

Figure 3. MRI T2 mapping (seconds); (**a**) before—with ROI's in the stratum corneum, epidermis and dermis; and (**b**) 1 h after moisturiser application [148].

Although most NMR studies evaluated the entire skin including the dermis, a report by Salter [149] and a similar one by Mirrashed and Sharp [150], visualised the hydration-dehydration process using MRI with a resolution of 0.6 mm after 1 h of skin occlusion. The brightness and SC thickness of the two layers were different depending on their hydration levels, and after some time, the outer band disappeared as the surface became dry. Thus, despite its expensive and complicated operation, MRI provides global analysis with high resolution of the various skin layers down to the hypodermis and the muscular fascia, and remains a valuable tool in skin-related research.

9. Optical Coherence Tomography

Optical Coherence Tomography (OCT) is an imaging technique that uses broadband near-IR light waves, and works by reconstructing a depth profile of a sample's structure using the time-delay information present in the light waves that were reflected from different depths inside the sample. A 3-dimensional image can then be produced by scanning a light beam laterally across the surface of

the sample. The lateral resolution is arbitrated by the spot size of the light beam, whereas the depth resolution relies primarily on the optical bandwidth of the radiation source. As a result, OCT methods can give high axial resolutions with large field depths, and are useful for in vivo imaging of thick sections of biological mediums.

OCT instrumentation come in two categories: Time-Domain OCT (TDOCT) or Spectral-Domain OCT (FDOCT or SDOCT). Early OCT systems were mostly based on TDOCT technology and used in earlier experiments. However, SDOCT is more sensitive and offers higher image acquisition speed, thereby rapidly replacing TDOCT in many applications.

For healthy skin measurements, OCT allows real-time in vivo imaging that is capable of distinguishing thickened layers of SC as shown in Figure 4, and can clearly identify the epidermis, the dermo-epidermal junction, as well as the normal regional differences and well defined anatomical sites [60,151–153]. The information acquired at each depth of skin is achieved by adjusting the reference beam path length by scanning with the mirror.

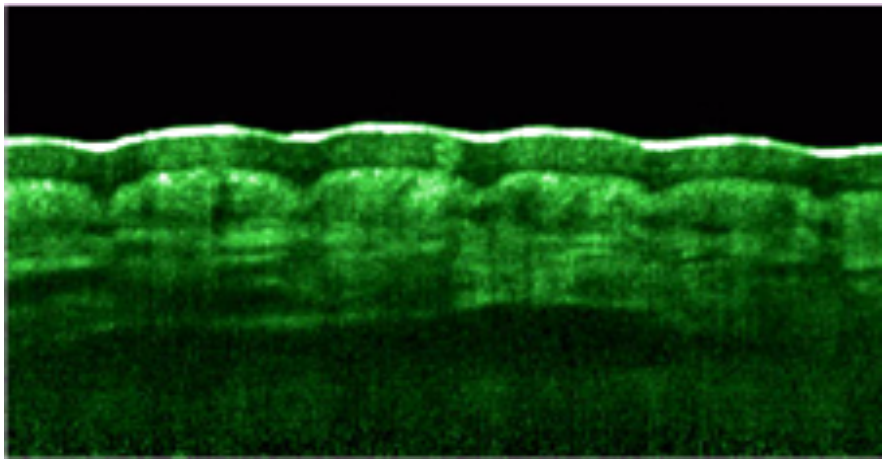

Figure 4. Speckle reduced OCT image obtained by combining 8 individual scans to suppress speckle noise. The SC is marked by the white-coloured top layer [154].

Due to short coherence length, spatial depth resolution can be less than 10 µm, but owing to multiple scattering, this can be restricted to reconnaissance depths of a few 100 µm, increasing accordingly with depth. Deeper exploration depths of >1 mm are attainable with a decline in resolution.

It was revealed by multiple studies [155–157] that by altering the focus of light in the measurement arm at different refractive index (n) of skin and if the focal point is found for varying lens configurations by analysing the acquired image data, n can be quantitatively reconstructed (Figure 4). In turn, the refractive index of skin is significantly linked to its water content, and so the technique can be used for skin hydration measurements. Knuttel et al. [157] extracted optical scattering properties using the Huygens-Fresnel model simultaneously with refractive index measurements, and related the effects of skin hydration levels to the optical characteristics retrieved from OCT images.

Furthermore, OCT has been extensively used in investigations of skin pathology including Nonmelanoma skin cancer [158–168], and inflammatory skin conditions such as contact dermatitis and psoriasis [151,167,169]. Welzel [151] applied OCT in patients suffering from contact dermatitis and psoriasis, and found that light scattering in the upper dermis was reduced in healthy skin, indicating that edema provided enhanced optical settings for imaging of collagen fibres. Although variations in OCT images did not entirely correlate with those shown by other methods, the technique can effectively determine epidermal thickness and the signal attenuation coefficient in the upper dermis in both skin conditions. The use of OCT for measurement of SC, epidermal and full skin thickness remains employed in current reports on the effects of topical moisturisers [170–172], and on skin ageing [173,174].

10. Raman Spectroscopy

When a ray of light becomes incident on a sample, several processes can occur. Light may travel through and remain unaltered, or it can be reflected or absorbed. It can also be scattered in different directions while maintaining its energy. The latter is known as elastic or Rayleigh scattering. Alternatively, light can undergo an inelastic scattering process, whereby energy is transferred to or from the medium, and the scattered photon has less or more energy than that of the incident photon. When the scattered photon has less energy, the process is known as Raman stokes scattering, while the opposite is referred to as Raman anti-stokes scattering. This is the mechanism of Raman scattering which forms the basis of Raman Spectroscopy (RS), and deals with the Raman Effect resulting from energy exchange between incident photons and molecular scattering.

Because Raman signals are generally weak, all commercial Raman spectrometers employ a laser as a source of radiation, accompanied by very sensitive detectors particularly in in vivo applications. Other essential components include a sampling stage and a spectrometer that separates and records the different frequency components. A typical output of a Raman spectrometer is a spectrum of scattered intensity versus the frequency shift between the incident and scattered photons. This frequency shift is proportional to the energy difference, and is distinctive of the molecule that the photon collided with. The final spectrum features a series of Raman bands that are consistent with the various vibrational modes of the sample molecule. Raman peaks are often spectrally narrow and mostly relate to the vibration of a specific molecular bond.

Most biological molecules are Raman-active and have fingerprint spectral properties. Therefore, Raman spectra include information pertaining to the molecular composition or chemical fingerprint, structure, phase, orientation, and even concentration of chemical substances, hence the technique is especially suited to studies of molecular composition in pathological skin [175–187].

Due to the natural fluorescence of mammalian skin presenting an obstacle in Raman spectroscopic measurements, it is only when longer wavelength near-IR excitation was developed that the technique was applied to the skin [188]. Earlier reports focused on identifying key Raman biomarkers that could be implemented to investigate skin molecular components, and the possibility of characterising healthy and diseased skin tissue [189]. Such reports included investigations into the state of skin hydration [190,191], on the role of skin NMFs [192–195], and the effects of UV protective agents, photoageing, and chronic ageing on water and protein structure [196,197].

The use of RS to examine lateral packing and conformational order of SC lipids is well established, as well as in evaluations of SC water profiles [198], and determinations of lipid/protein ratio through calculations of lipid and protein intensity peaks [199]. Such attributes have been employed in a variety of skin-related studies of barrier permeability in dry skin conditions [199–202], substance penetration [203], and evaluations of the efficacy of moisturisers [204] and anti-ageing ingredients and formulations [56,205].

11. Confocal Raman Microscopy

Confocal Raman Microscopy (CRM), also termed Confocal Raman Spectroscopy, combines a Raman spectrometer and a standard optical microscope, together offering highly magnified sample visualisation as well as Raman analysis with a microscopic laser spot. The arrangement includes a spatial filter, which enables spatial filtering of the analysis volume of the sample in the xy (lateral) and z (depth) axes. This makes it possible to analyse individual particles or layers with dimensions down to 1 µm and below.

For an ideal confocal design, the extents of spatial resolution are illustrated principally by the laser wavelength, the quality of the employed laser beam, and the selected type of microscope objective. As this poses a significant technical challenge, it was some time before commercial instruments suitable for skin measurements became available, the first being the Raman skin analyzer® 3510 (RiverD International B.V., Rotterdam, The Netherlands).

In recent years, CRM has gained much interest and is considered a powerful technique in biomolecular analysis that can directly measure skin molecular composition and structure, and allow acquisition of depth profiles of SC and deeper skin layers. In relation to skin hydration, the first series of studies were carried out by Caspers et al. [192–195] who performed in vivo studies of human skin, and demonstrated the variations in water concentration within the SC and epidermis at penetration depths of up to 100 μm (Figure 5). The same author investigated skin components that produced Raman signals [193], and reported temporal and spatial changes for the penetration-enhancer dimethyl sulfoxide in the SC [192]. Moreover, the technique allowed construction of water concentration profiles of human SC with obvious consequences for penetration of exogenous hydrophilic molecules [193,206,207].

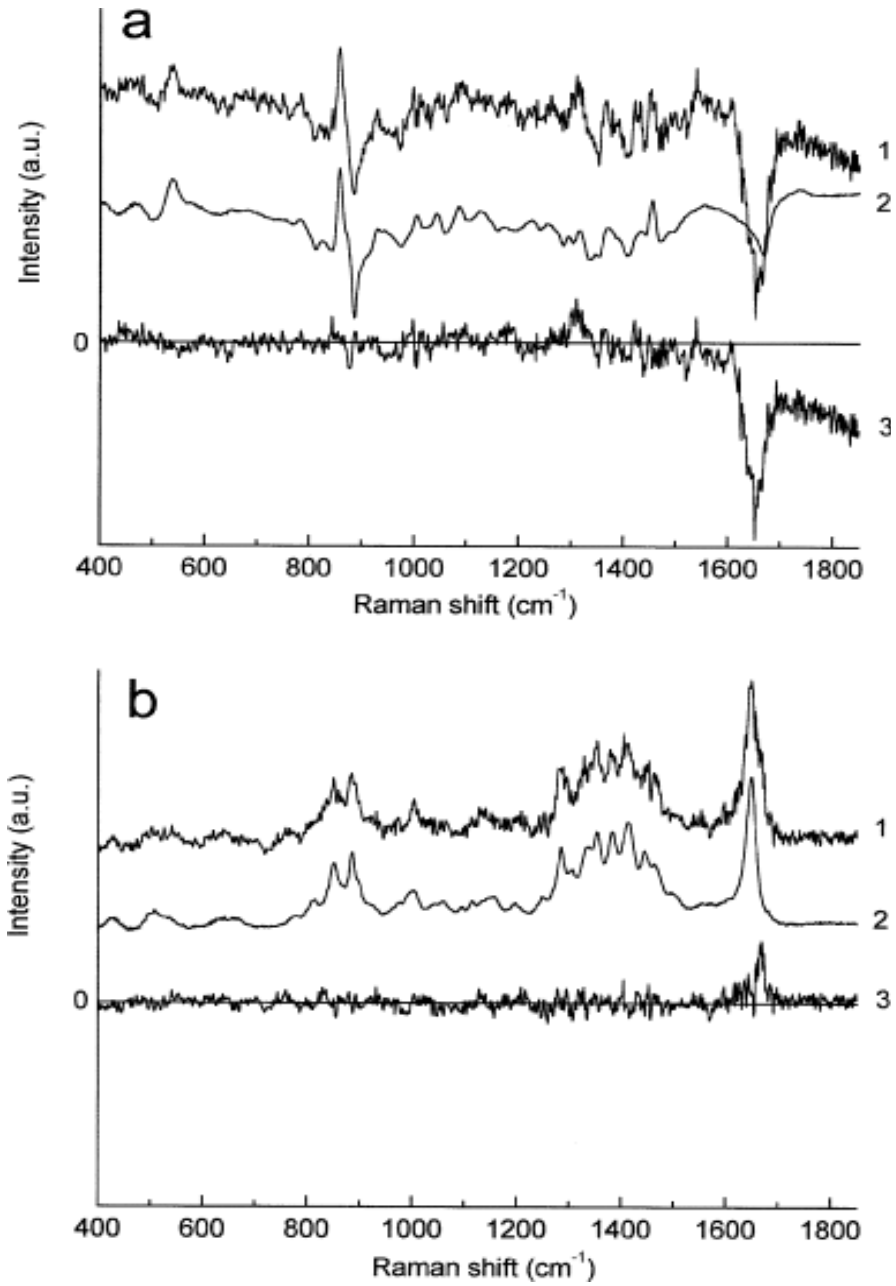

Figure 5. Raman spectra obtained at different depths below the skin surface by means of the qualitative least-squares fit. (**a**) (1) Difference between Raman spectra obtained at the skin surface and at 10 μm below; (2) fit result; (3) residual (curve 1–curve 2). (**b**) (1) Difference between Raman spectra obtained at 60 μm and 70 μm below skin surface; (2) fit result; (3) residual (curve 1–curve 2) [193].

Further studies from cosmetics research focused on the effects of moisturising ingredients and the ability to monitor Raman-active molecules which have been topically applied on the skin, to study the evolution in time of concentration profiles. One performed by Sieg et al. [208] compared the efficacy of three different moisturisers in vivo over a period of 3 weeks. The obtained Raman spectra were used to build concentration profiles of water and NMFs, and the thickness of SC was determined at different anatomic sites from the water concentration profiles.

Furthermore, evaluations of intercellular lipids packing and ordering, and SC thickness are commonly performed using CRM [209–214], and include applications in skin ageing [211,212] and topical oils [209]. Eklouh-Molinier [211] combined CRM and cutometric data into a Partial Least-Squares (PLS) model in an attempt to profile spectral markers associated with ageing, and used this to create a "biological age" chart that mapped skin age based on its molecular state rather than its chronological age. Besides SC thickness and water content, measurements of ceramides/fatty acids and NMF content are possible with CRM, and can be used to assess barrier function [215,216], as well as the penetration of sunscreens [217,218], cosmetic ingredients [219–221], and other substances [220,222–228].

Overall, CRM is finding increasing use in the characterisation of skin in biomedical, pharmaceutical and cosmetic studies, and further optimisation of its instrumentation and data analysis [229,230] are likely to reinforce its employment in skin-related applications.

12. Near Infrared Spectroscopy

Near Infrared (NIR) Spectroscopy is a subset of IR spectroscopy that addresses the broad and less intense peaks in the NIR region between 750–2500 nm of the electromagnetic spectrum. Unlike mid-IR measurements, NIR spectroscopy is capable of deeper sample penetrations and gives the absorptivity of the given species based on its molecular overtone and combination vibrations.

Nonetheless, due to the broad nature of these vibrations and the complexity of NIR spectra, it is difficult to assign specific attributes to a definite chemical component, and therefore, multivariate calibrations techniques such as Principal Component Analysis (PCA), PLS, or Artificial Neural Networks (ANN) are often necessary to extract relevant information.

A typical NIR spectrum of skin contains absorption bands related to water, and their intensity directly proportional to skin water content. NIR spectra can differentiate the types of water present inside the SC, as demonstrated by Martin [231], who applied diffuse reflectance NIR and found four types of water to exist. These were: water linked to the lipid phase within the SC, bulk water, secondary water, and primary water.

NIRS was used in several studies determining SC water contents at multiple anatomical sites [232–237], while several others focused on the characterization of dry skin. Characterization of skin lesions and tumours [238–240] were also investigated in cancer-related studies, but a limited number of reports are available regarding spongiotic disorders. Dreassi et al. [241–243], published a series of reports on atopic skin, where pattern recognition statistics were combined with reflectance NIRS and showed that it was possible to differentiate between atopic and healthy samples and between the different fomblins that were applied. Works on skin characterisation were performed on healthy skin [244], and on pathological skin e.g., scoring the severity of psoriasis conditions [245].

More popular, are studies testing the efficacy of moisturising formulations to answer the question of whether skin which appeared dry was in fact low in water [233,246,247]. Arimoto and Egawa [234] performed in vivo and in vitro measurements and compared NIR spectroscopic data with the capacitance method. They also used multivariate analysis and Monte Carlo simulation to fit NIR data, and reported that the sampling depth was strongly dependent on water absorption in the spectral region between 1250–2500 nm, and that NIRS monitors water from regions deeper than the capacitance method. Moreover, the same group [237], as well as Mohamad et al. [248] conducted experiments on regional differences of water content [237]. The former assumed that regional differences relied on sampling depths, variations in skin surface reflection and SC thickness.

All spectra obtained from previous reports showed the peak characteristics of water near 1940 and 1450 nm. Wirchrowski & Khaiat [249] expressed the absorbance at 1940 nm as a function of a reference absorption at 1100 nm in isolated samples of SC placed under increasingly controlled humidity settings. These results correlated well with those reported by Abuzahra & Baron [158] using OCT, which signified the absorbance at 1940 nm as relative to a reference at 1850 nm.

Skin spectra acquired in vitro by De Rigal et al. [4,246] showed that the dermis alone had a much larger absorbance compared to the remainder of skin, probably due to its larger volume, a decrease in surface diffusion and the elimination of the less hydrated layer. The same investigation of dry skin [246] first carried out a visual assessment of the legs of participants prior to measurements and gave each a score between 1 and 5. Each given score was then compared to acquired spectra, and clearly indicated that absorbance decreased with the severity of dry skin condition. The study also compared the efficacy of five daily cosmetic treatments over a period of 4 weeks. Walling [233] concluded that after calibration, it was possible to use NIRS to predict the score of dry skin.

Finally, a series of studies by Qassem et al. [250–253] combined NIR data with both PCR and PLS techniques and found clear spectral differences associated with frequency of moisturiser use (Figure 6), and highlighted the possibility of using this technique to detect changes in barrier function by measuring water penetration after wet patch testing. The authors suggested that NIR spectroscopy can provide comprehensive skin analysis in a fast and simple manner.

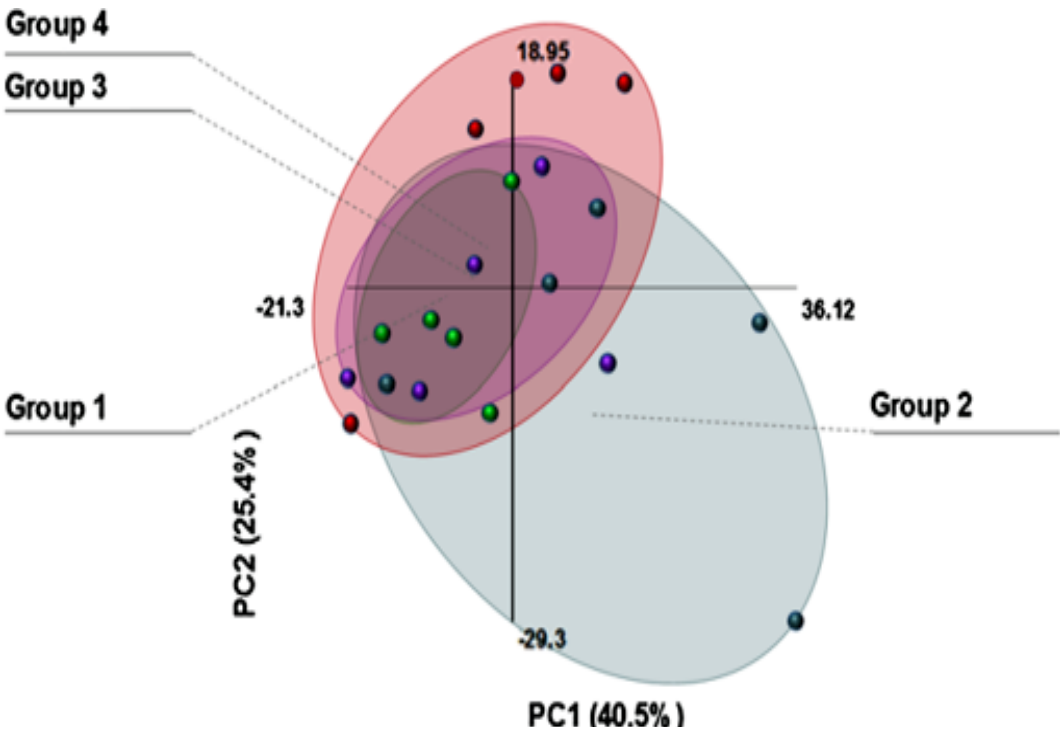

Figure 6. Scores plot of PCA analysis of NIR spectra acquired from individuals with varied moisturizing patterns. (Group 1) daily, (Group 2) none, (Group 3) daily & dry skin, and (Group 4) random. Vairability indicated by size of oval grouping [250].

13. Discussion

Traditional methods such as capacitance, TEWL and mechanical-based techniques are considered the standard in skin-related measurements, and use SC water content as a primary factor in determining SC hydration and barrier function without precisely analysing its composition nor its structure. However, it is important to evaluate additional skin parameters such as lipid and protein compositions to truly understand the phenomena quantified by indirect methods that are normally used, and monitor

the efficacy of various formulations applied on the skin. For this purpose, several spectroscopic and imaging techniques have been employed in recent years.

Capacitance/resistance measuring probes that determine skin moisture by means of skin conductivity or impedance are often occlusive, which can lead to inaccuracies resulting from water build up on the examination site [131], and according to their theory of operation, the flow of electrical current through the SC is associated with its water content, but this flow is also influenced by alterations in ion movement and by re-orientation of protein dipole moments. Therefore, the presence of salts from formulations or perspiration can impact ion mobility, and other chemicals can disrupt the protein arrangement, thereby modifying the orientation of protein dipole moments. Besides their principal drawbacks, electrical-based devices provide arbitrary outputs, without further details on additional factors that influence this parameter, though their quick operation is beneficial in many settings.

Similarly, TEWL and mechanical-based devices have proved excellent in highlighting the biomechanical nature of SC, but nonetheless, they do not provide direct measurements of skin hydration or barrier function and merely serve as indicators of changes in these parameters.

In recent years, the availability of spectroscopic and imaging techniques suitable for skin measurements has placed greater interest on detailed analysis of skin structure and composition in relation to skin hydration and barrier function. Prior to this, evaluations of the state of SC water and characterisation of SC water types were only possible using DSC, which remains the standard but involves complex and time-consuming procedures, and only feasible for ex vivo measurements. Furthermore, emerging techniques such as multimodal sensors of skin hydration [254–256] claim to offer "skin-like" devices that integrate with skin without application of pressure for real-time, in vivo hydration assessment but these remain in early research.

Spectroscopic techniques such as OTTER, IR, NIR, and Raman are well established for skin-related measurements and enable assessment of multiple attributes including SC thickness, water concentration gradient within the SC, and lipid molecular organisation. This is the same for imaging techniques such as MRI, OCT, and CRM, which can provide clear images of skin layers and constituents that encompass structural details on morphology, thickness, and water content. CRM is even able to establish water concentration profiles of skin in regions such as the palms and forearm, with a 5 cm^{-1} resolution and up to 100 mm in depth.

The mentioned spectroscopic and imaging techniques are capable of direct measurements, but due to the complex nature of acquired data, advanced data analysis techniques e.g., multivariate methods, are often necessary, though their primary limitations are the expensive costs of instrumentation, and as most are bench-top instruments, measurements are restricted to specific anatomical sites. Exceptions to this are NIR spectroscopy and OTTER. NIR spectroscopic instrumentation can be easily coupled with flexible fibre optics and portable spectrometers for reduced costs and restrictions on selection of examination site, and can offer increased stability against environmental conditions such as temperature and relative humidity [248,250,257]. Moreover, techniques such as ATR-IR are occlusive, which can cause accumulation of water at the test site, and as for OCT, the coherence length is short, and resolution can be less than 10 µm. Despite their limitations, sophisticated spectroscopic and imaging techniques provide detailed analysis of various skin attributes, and although traditional methods remain employed, they are now commonly accompanied by spectral or imaging data for comprehensive assessment of skin.

Author Contributions: Conceptualization, M.Q.; investigation, M.Q.; data curation, M.Q.; writing–original draft preparation, M.Q.; writing–review and editing, M.Q. and P.K.; supervision, P.K.; project administration, P.K.

Funding: This research received no external funding.

Conflicts of Interest: The authors declare no conflict of interest.

Abbreviations

The following abbreviations are used in this manuscript:

SC	Stratum Corneum
RH	Relative Humidity
DSC	Differential Scanning Calorimetry
SCIM	Surface-Characterizing Impedance monitor
TEWL	Transepidermal Water Loss
OTTER	Opto-Thermal Transient Emission Radiometry
WVFD	Water vapor flux density
ATR-IR	Attenuated Total Reflection Infrared
ATR-FTIR	Attenuated Total Reflection Fourier Transform Infrared
IRE	Internal Reflectance Element
NMR	Nuclear Magnetic Resonance
MRI	Magnetic Resonance imaging
OCT	Optical Coherence Tomography
TDOCT	Time-Domain Optical Coherence Tomography
SDOCT	Spectral-Domain Optical Coherence Tomography
RS	Raman Spectroscopy
CRM	Confocal Raman Microscopy
PLS	Partial Least-Squares
NIR	Near Infrared
PCA	Principal Component Analysis
ANN	Artificial Neural Networks

References

1. Marieb, E.N.; Mallatt, J. *Human Anatomy*, 2nd ed.; Benjamin-Cummings Pub Co.: San Francisco, CA, USA, 1996.
2. Leyden, J.J.; Rawlings, A.V. *Skin Moisturization*, 1st ed.; Informa Healthcare: London, UK, 2002.
3. Chiu, M.H.; Prenner, E.J. Differential scanning calorimetry: An invaluable tool for a detailed thermodynamic characterization of macromolecules and their interactions. *J. Pharm. Bioallied Sci.* **2011**, *3*, 39–59. [CrossRef] [PubMed]
4. Agache, P.G.; Humbert, P.; Maibach, H.I. *Measuring the Skin*; Springer: Berlin, Germany, 2004.
5. Golden, G.M.; Guzek, D.B.; Harris, R.R.; McKie, J.E.; Potts, R.O. Lipid thermotropic transitions in human stratum corneum. *J. Investig. Dermatol.* **1986**, *86*, 255–259. [CrossRef]
6. Khan, Z.; Kellaway, I. Differential scanning calorimetry of dimethylsulphoxide-treated human stratum corneum. *Int. J. Pharm.* **1989**, *55*, 129–134. [CrossRef]
7. Golden, G.M.; Guzek, D.B.; Kennedy, A.H.; McKie, J.E.; Potts, R.O. Stratum corneum lipid phase transitions and water barrier properties. *Biochemistry* **1987**, *26*, 2382–2388. [CrossRef] [PubMed]
8. Barry, B. Mode of action of penetration enhancers in human skin. *J. Control. Release* **1987**, *6*, 85–97. [CrossRef]
9. Potts, R.O.; Golden, G.M.; Francoeur, M.L.; Mak, V.H.; Guy, R.H. Mechanism and enhancement of solute transport across the stratum corneum. *J. Control. Release* **1991**, *15*, 249–260. [CrossRef]
10. Al-Saidan, S.; Barry, B.; Williams, A. Differential scanning calorimetry of human and animal stratum corneum membranes. *Int. J. Pharm.* **1998**, *168*, 17–22. [CrossRef]
11. Papir, Y.S.; Hsu, K.H.; Wildnauer, R.H. The mechanical properties of stratum corneum. I. The effect of water and ambient temperature on the tensile properties of newborn rat stratum corneum. *Biochim. Biophys. Acta* **1975**, *399*, 170–180. [CrossRef]
12. Miller, D.L.; Wildnauer, R.H. Thermoanalytical probes for the analysis of physical properties of stratum corneum. *J. Investig. Dermatol.* **1977**, *69*, 287–289. [CrossRef]
13. Inoue, T.; Tsujii, K.; Okamoto, K.; Toda, K. Differential scanning calorimetric studies on the melting behavior of water in stratum corneum. *J. Investig. Dermatol.* **1986**, *86*, 689–693. [CrossRef]
14. Imokawa, G.; Kuno, H.; Kawai, M. Stratum Corneum Lipids Serve as a Bound-Water Modulator. *J. Investig. Dermatol.* **1991**, *96*, 845–851. [CrossRef] [PubMed]

15. Perez, B.; Dahlgaard, S.E.; Bulsara, P.; Rawlings, A.V.; Jensen, M.M.; Dong, M.; Glasius, M.; Clarke, M.J.; Guo, Z. Synthesis and characterization of O-acylated-ω-hydroxy fatty acids as skin-protecting barrier lipids. *J. Colloid Interface Sci.* **2017**, *490*, 137–146. [CrossRef] [PubMed]
16. Perez, B.; Hansen, B.S.; Bulsara, P.A.; Rawlings, A.V.; Clarke, M.J.; Guo, Z. Fractionated aliphatic alcohols as synthetic precursors of ultra long-chain monoacylglycerols for cosmetic applications. *Int. J. Cosmet. Sci.* **2017**, *39*, 511–517. [CrossRef]
17. Libio, I.C.; Demori, R.; Ferrão, M.F.; Lionzo, M.I.Z.; da Silveira, N.P. Films based on neutralized chitosan citrate as innovative composition for cosmetic application. *Mater. Sci. Eng. C Mater. Biol. Appl.* **2016**, *67*, 115–124. [CrossRef]
18. Täuber, A.; Müller-Goymann, C.C. In vitro model of infected stratum corneum for the efficacy evaluation of poloxamer 407-based formulations of ciclopirox olamine against Trichophyton rubrum as well as differential scanning calorimetry and stability studies. *Int. J. Pharm.* **2015**, *494*, 304–311. [CrossRef]
19. Gazga-Urioste, C.; Rivera-Becerril, E.; Pérez-Hernández, G.; Angélica Noguez-Méndez, N.; Faustino-Vega, A.; Tomás Quirino-Barreda, C. Physicochemical characterization and thermal behavior of hexosomes containing ketoconazole as potential topical antifungal delivery system. *Drug Dev. Ind. Pharm.* **2018**, 1–9. [CrossRef] [PubMed]
20. Rubio, L.; Alonso, C.; Rodríguez, G.; Cócera, M.; Barbosa-Barros, L.; Coderch, L.; de la Maza, A.; Parra, J.L.; López, O. Bicellar systems as vehicle for the treatment of impaired skin. *Eur. J. Pharm. Biopharm.* **2014**, *86*, 212–218. [CrossRef]
21. Montenegro, L.; Castelli, F.; Sarpietro, M.G. Differential Scanning Calorimetry Analyses of Idebenone-Loaded Solid Lipid Nanoparticles Interactions with a Model of Bio-Membrane: A Comparison with In Vitro Skin Permeation Data. *Pharmaceuticals* **2018**, *11*, 138. [CrossRef]
22. Ansari, H.; Singh, P. Formulation and in-vivo Evaluation of Novel Topical Gel of Lopinavir for Targeting HIV. *Curr. HIV Res.* **2018**. [CrossRef]
23. Pireddu, R.; Sinico, C.; Ennas, G.; Schlich, M.; Valenti, D.; Murgia, S.; Marongiu, F.; Fadda, A.M.; Lai, F. The effect of diethylene glycol monoethyl ether on skin penetration ability of diclofenac acid nanosuspensions. *Colloids Surf. B Biointerfaces* **2018**, *162*, 8–15. [CrossRef]
24. Lauterbach, A.; Mueller-Goymann, C.C. Development, formulation, and characterization of an adapalene-loaded solid lipid microparticle dispersion for follicular penetration. *Int. J. Pharm.* **2014**, *466*, 122–132. [CrossRef] [PubMed]
25. Walters, K.A.; Roberts, M.S. *Dermatologic, Cosmeceutic, and Cosmetic Development: Therapeutic and Novel Approaches*, 1st ed.; CRC Press: Boca Raton, FL, USA, 2007.
26. Pierard, G. Skin capacitance imageing for the dermatologist. *Dermatology* **2005**, *210*, 3–7.
27. Batisse, D.; Giron, F.; Lévêque, J.L. Capacitance imageing of the skin surface. *Skin Res. Technol.* **2006**, *12*, 99–104. [CrossRef] [PubMed]
28. Lévêque, J.L.; Querleux, B. SkinChip, a new tool for investigating the skin surface in vivo. *Skin Res. Technol.* **2003**, *9*, 343–347. [CrossRef] [PubMed]
29. Leveque, J.L.; Xhauflaire-Uhoda, E.; Pierard, G.E. Skin capacitance imageing, a new technique for investigating the skin surface. *Eur. J. Dermatol.* **2006**, *16*, 500–506. [PubMed]
30. Diridollou, S.; de Rigal, J.; Querleux, B.; Leroy, F.; Holloway Barbosa, V. Comparative study of the hydration of the stratum corneum between four ethnic groups: Influence of age. *Int. J. Dermatol.* **2007**, *46* (Suppl. 1), 11–14. [CrossRef] [PubMed]
31. Crowther, J.M. Understanding the effects of topography on skin moisturization measurement via two-dimensional capacitance imageing. *Int. J. Cosmet. Sci.* **2017**, *39*, 572–578. [CrossRef] [PubMed]
32. Xhauflaire-Uhoda, E.; Pierard-Franchimont, C.; Pierard, G.E. Skin capacitance mapping of psoriasis. *J. Eur. Acad. Dermatol. Venereol.* **2006**, *20*, 1261–1265. [CrossRef]
33. Pierard-Franchimont, C.; Pierard, G. Sweat Gland Awakening on Physical Training: A Skin Capacitance Mapping Observation. *Clin. Res. Dermatol.* **2015**, *2*, 1–4. [CrossRef]
34. Klang, V.; Schwarz, J.C.; Haberfeld, S.; Xiao, P.; Wirth, M.; Valenta, C. Skin integrity testing and monitoring of in vitro tape stripping by capacitance-based sensor imageing. *Skin Res. Technol.* **2013**, *19*, e259–e272. [CrossRef]

35. Xhauflaire-Uhoda, E.; Mayeux, G.; Quatresooz, P.; Scheen, A.; Pierard, G.E. Facing up to the imperceptible perspiration. Modulatory influences by diabetic neuropathy, physical exercise and antiperspirant. *Skin Res. Technol.* **2011**, *17*, 487–493. [CrossRef] [PubMed]
36. Xhauflaire-Uhoda, E.; Pierard-Franchimont, C.; Pierard, G.E.; Quatresooz, P. Weathering of the hairless scalp: A study using skin capacitance imageing and ultraviolet light-enhanced visualization. *Clin. Exp. Dermatol.* **2010**, *35*, 83–85. [CrossRef] [PubMed]
37. Leveque, J.L.; Goubanova, E. Influence of age on the lips and perioral skin. *Dermatology* **2004**, *208*, 307–313. [CrossRef] [PubMed]
38. Xhauflaire-Uhoda, E.; Pierard, G.E. Skin capacitance imageing of acne lesions. *Skin Res. Technol.* **2007**, *13*, 9–12. [CrossRef] [PubMed]
39. Xhauflaire-Uhoda, E.; Loussouarn, G.; Haubrechts, C.; Leger, D.S.; Pierard, G.E. Skin capacitance imageing and corneosurfametry. A comparative assessment of the impact of surfactants on stratum corneum. *Contact Dermat.* **2006**, *54*, 249–253. [CrossRef] [PubMed]
40. Zhang, X.; Bontozoglou, C.; Chirikhina, E.; Lane, M.E.; Xiao, P. Capacitive Imageing for Skin Characterizations and Solvent Penetration Measurements. *Cosmetics* **2018**, *5*, 52. [CrossRef]
41. Berardesca, E.; Loden, M.; Serup, J.; Masson, P.; Rodrigues, L.M. The revised EEMCO guidance for the in vivo measurement of water in the skin. *Skin Res. Technol.* **2018**, *24*, 351–358. [CrossRef]
42. Gefen, A. *Bioengineering Research of Chronic Wounds: A Multidisciplinary Study Approach*; Springer: Berlin, Germany, 2009.
43. Farahmand, S.; Tien, L.; Hui, X.; Maibach, H.I. Measuring transepidermal water loss: A comparative in vivo study of condenser-chamber, unventilated-chamber and open-chamber systems. *Skin Res. Technol.* **2009**, *15*, 392–398. [CrossRef]
44. Nuutinen, J.; Alanen, E.; Autio, P.; Lahtinen, M.R.; Harvima, I.; Lahtinen, T. A closed unventilated chamber for the measurement of transepidermal water loss. *Skin Res. Technol.* **2003**, *9*, 85–89. [CrossRef]
45. Chilcott, R.; Price, S. *Principles and Practice of Skin Toxicology*; John Wiley & Sons: Hoboken, NJ, USA, 2008.
46. De Paepe, K.; Houben, E.; Adam, R.; Wiesemann, F.; Rogiers, V. Validation of the VapoMeter, a closed unventilated chamber system to assess transepidermal water loss vs. the open chamber Tewameter. *Skin Res. Technol.* **2005**, *11*, 61–69. [CrossRef]
47. Zhai, H.; Wilhelm, K.P.; Maibach, H.I. *Marzulli and Maibach's Dermatotoxicology*, 7th ed.; CRC Press: Boca Raton, FL, USA, 2007.
48. Bennett, S.; Jones, C.; Matheson, J.R. Closed chamber and open chamber TEWL measurements: A comparison of Dermalab(R) and Aquaflux AF102 instruments. In Proceesings of the 2005 World Congress on Noninvasive Studies of the Skin, Wilmington, DE, USA, 28 September–1 October 2005; p. 46.
49. Tian, W. Comparison of three TEWL instruments for in vitro and in vivo measurements. In Proceedings of the 2005 World Congress onNoninvasive Studies of the Skin, Wilmington, DE, USA, 28 September–1 October 2005; p. 75.
50. Rogiers, V.; EEMCO Group. EEMCO guidance for the assessment of transepidermal water loss in cosmetic sciences. *Skin Pharmacol. Appl. Skin Physiol.* **2001**, *14*, 117–128. [CrossRef] [PubMed]
51. Zhang, Z.; Lukic, M.; Savic, S.; Lunter, D.J. Reinforcement of barrier function—Skin repair formulations to deliver physiological lipids into skin. *Int. J. Cosmet. Sci.* **2018**, *40*, 494–501. [CrossRef] [PubMed]
52. De Paepe, K.; Roseeuw, D.; Rogiers, V. Repair of acetone- and sodium lauryl sulphate-damaged human skin barrier function using topically applied emulsions containing barrier lipids. *J. Eur. Acad. Dermatol. Venereol.* **2002**, *16*, 587–594. [CrossRef] [PubMed]
53. Chiba, T.; Nakahara, T.; Kohda, F.; Ichiki, T.; Manabe, M.; Furue, M. Measurement of trihydroxy-linoleic acids in stratum corneum by tape-stripping: Possible biomarker of barrier function in atopic dermatitis. *PLoS ONE* **2019**, *14*, e0210013. [CrossRef] [PubMed]
54. Lunnemann, L.; Ludriksone, L.; Schario, M.; Sawatzky, S.; Stroux, A.; Blume-Peytavi, U.; Garcia Bartels, N. Noninvasive monitoring of plant-based formulations on skin barrier properties in infants with dry skin and risk for atopic dermatitis. *Int. J. Women's Dermatol.* **2018**, *4*, 95–101. [CrossRef]
55. Yang, J.E.; Ngo, H.T.T.; Hwang, E.; Seo, S.A.; Park, S.W.; Yi, T.H. Dietary enzyme-treated Hibiscus syriacus L. protects skin against chronic UVB-induced photoageing via enhancement of skin hydration and collagen synthesis. *Arch. Biochem. Biophys.* **2019**, *662*, 190–200. [CrossRef] [PubMed]

56. Sundaram, H.; Mackiewicz, N.; Burton, E.; Peno-Mazzarino, L.; Lati, E.; Meunier, S. Pilot Comparative Study of the Topical Action of a Novel, Crosslinked Resilient Hyaluronic Acid on Skin Hydration and Barrier Function in a Dynamic, Three-Dimensional Human Explant Model. *J. Drugs Dermatol.* **2016**, *15*, 434–441.
57. Zheng, Y.; Chen, H.; Lai, W.; Xu, Q.; Liu, C.; Wu, L.; Maibach, H.I. Cathepsin D repairing role in photodamaged skin barrier. *Skin Pharmacol. Physiol.* **2015**, *28*, 97–102. [CrossRef]
58. Calabro, G.; De Vita, V.; Patalano, A.; Mazzella, C.; Lo Conte, V.; Antropoli, C. Confirmed efficacy of topical nifedipine in the treatment of facial wrinkles. *J. Dermatol. Treat.* **2014**, *25*, 319–325. [CrossRef]
59. Campos, P.M.B.G.M.; Gonçalves, G.M.S.; Gaspar, L.R. In vitro antioxidant activity and in vivo efficacy of topical formulations containing vitamin C and its derivatives studied by non-invasive methods. *Skin Res. Technol.* **2008**, *14*, 376–380. [CrossRef]
60. Baran, R. *Textbook of Cosmetic Dermatology*; CRC Press: Boca Raton, FL, USA, 2005.
61. Escoffier, C.; de Rigal, J.; Rochefort, A.; Vasselet, R.; Lévêque, J.L.; Agache, P.G. Age-related mechanical properties of human skin: An in vivo study. *J. Investig. Dermatol.* **1989**, *93*, 353–357. [CrossRef]
62. Both, W.; Busch, P. Torsion measurement as a means of assessing skin characteristics. In Proceedings of the Forum Cosmeticum Basel, Basel, Switzerland, 19–20 February 1998; pp. 238–250.
63. Laden, K.; Morrow, R. Torsional measurements on skin. *J. Soc. Cosmet. Chem.* **1970**, *21*, 417.
64. Leveque, J.L.; De Rigal, J. In vivo measurements of the stratum corneum elasticity. *Bioeng. Skin* **1985**, *1*, 13–23.
65. Wiechers, J.W. A supplier's contribution to performance testing of personal care ingredients. *Sofw. Seifen Ole Fette Wachse* **1997**, *123*, 981–990.
66. Berardesca, E.; de Rigal, J.; Leveque, J.L.; Maibach, H.I. In vivo biophysical characterization of skin physiological differences in races. *Dermatologica* **1991**, *182*, 89–93. [CrossRef]
67. Rawlings, A.V. Ethnic skin types: Are there differences in skin structure and function? *Int. J. Cosmet. Sci.* **2006**, *28*, 79–93. [CrossRef]
68. Tur, E. Physiology of the skin–differences between women and men. *Clin. Dermatol.* **1997**, *15*, 5–16. [CrossRef]
69. Batisse, D.; Bazin, R.; Baldeweck, T.; Querleux, B.; Leveque, J.L. Influence of age on the wrinkling capacities of skin. *Skin Res. Technol.* **2002**, 148–154. [CrossRef]
70. Salter, D.; McArthur, H.; Crosse, J.; Dickens, A. Skin mechanics measured in vivo using torsion: A new and accurate model more sensitive to age, sex and moisturizing treatment. *Int. J. Cosmet. Sci.* **1993**, *15*, 200–218. [CrossRef]
71. Sanders, R. Torsional elasticity of human skin in vivo. *Pflügers Archiv Eur. J. Physiol.* **1973**, *342*, 255–260. [CrossRef]
72. Leveque, J.L.; Corcuff, P.; de Rigal, J.; Agache, P. In Vivo Studies of the Evolution of Physical Properties of the Human Skin with Age. *Int. J. Dermatol.* **1984**, *23*, 322–329. [CrossRef] [PubMed]
73. Hara, Y.; Masuda, Y.; Hirao, T.; Yoshikawa, N. The relationship between the Young's modulus of the stratum corneum and age: A pilot study. *Skin Res. Technol.* **2013**, *19*, 339–345. [CrossRef]
74. Baumann, L. *Cosmetic Dermatology: Principles and Practice*; McGraw-Hill Prof Med/Tech: New York, NY, USA, 2009.
75. Nedelec, B.; Couture, M.A.; Calva, V.; Poulin, C.; Chouinard, A.; Shashoua, D.; Gauthier, N.; Correa, J.A.; de Oliveira, A.; Mazer, B.; et al. Randomized controlled trial of the immediate and long-term effect of massage on adult postburn scar. *Burns J. Int. Soc. Burn Inj.* **2019**, *45*, 128–139. [CrossRef] [PubMed]
76. Moortgat, P.; Meirte, J.; Maertens, K.; Lafaire, C.; De Cuyper, L.; Anthonissen, M. Can a cohesive silicone bandage outperform an adhesive silicone gel sheet in the treatment of scars? A randomised comparative trial. *Plast. Reconstr. Surg.* **2018**. [CrossRef]
77. Cortes, H.; Magana, J.J.; Reyes-Hernandez, O.D.; Zacaula-Juarez, N.; Gonzalez-Torres, M.; Diaz-Beltrán, W.; León-Trejo, M.C.; Cariño-Calvo, L.; Leyva-Gómez, G.; González-Del Carmen, M. Non-invasive analysis of skin mechanical properties in patients with lamellar ichthyosis. *Skin Res. Technol.* **2019**. [CrossRef] [PubMed]
78. Mazzarello, V.; Ferrari, M.; Ena, P. Werner syndrome: Quantitative assessment of skin ageing. *Clin. Cosmet. Investig. Dermatol.* **2018**, *11*, 397–402. [CrossRef]
79. Busche, M.N.; Thraen, A.C.J.; Gohritz, A.; Rennekampff, H.O.; Vogt, P.M. Burn Scar Evaluation Using the Cutometer® MPA 580 in Comparison to "Patient and Observer Scar Assessment Scale" and "Vancouver Scar Scale". *J. Burn Care Res.* **2018**, *39*, 516–526. [CrossRef]

80. Gardien, K.L.M.; Marck, R.E.; Bloemen, M.C.T.; Waaijman, T.; Gibbs, S.; Ulrich, M.M.W.; Middelkoop, E.; Dutch Outback Study Group. Outcome of Burns Treated With Autologous Cultured Proliferating Epidermal Cells: A Prospective Randomized Multicenter Intrapatient Comparative Trial. *Cell Transplant.* **2016**, *25*, 437–448. [CrossRef]
81. Hansen, B.; Jemec, G.B.E. The mechanical properties of skin in osteogenesis imperfecta. *Arch. Dermatol.* **2002**, *138*, 909–911. [CrossRef]
82. Nedelec, B.; Correa, J.A.; de Oliveira, A.; Lasalle, L.; Perrault, I. Longitudinal burn scar quantification. *Burns J. Int. Soc. Burn Inj.* **2014**. [CrossRef]
83. Yoon, H.S.; Baik, S.H.; Oh, C.H. Quantitative measurement of desquamation and skin elasticity in diabetic patients. *Skin Res. Technol.* **2002**, *8*, 250–254. [CrossRef] [PubMed]
84. Nam, G.W.; Baek, J.H.; Koh, J.S.; Hwang, J.K. The seasonal variation in skin hydration, sebum, scaliness, brightness and elasticity in Korean females. *Skin Res. Technol.* **2014**. [CrossRef]
85. Bae, S.H.; Park, J.J.; Song, E.J.; Lee, J.A.; Byun, K.S.; Kim, N.S.; Moon, T.K. The comparison of the melanin content and UV exposure affecting ageing process: Seven countries in Asia. *J. Cosmet. Dermatol.* **2016**, *15*, 335–342. [CrossRef] [PubMed]
86. Coumare, R.; Bouten, L.; Barbier, F. Influence of the menstrual cycle on breast skin elasticity. *Comput. Methods Biomech. Biomed. Eng.* **2015**, *18* (Suppl. 1), 1912–1913. [CrossRef] [PubMed]
87. Song, E.J.; Lee, J.A.; Park, J.J.; Kim, H.J.; Kim, N.S.; Byun, K.S.; Choi, G.S.; Moon, T.K. A study on seasonal variation of skin parameters in Korean males. *Int. J. Cosmet. Sci.* **2015**, *37*, 92–97. [CrossRef] [PubMed]
88. Jemec, G.B.; Gniadecka, M.; Jemec, B. Measurement of skin mechanics: A study of inter- and intra-individual variation using the Dermaflex A. *Skin Res. Technol.* **1996**, *2*, 164–166. [CrossRef] [PubMed]
89. Jacobs, S.W.; Culbertson, E.J. Effects of Topical Mandelic Acid Treatment on Facial Skin Viscoelasticity. *Facial Plast. Surg.* **2018**, *34*, 651–656. [CrossRef]
90. Lapatina, N.G.; Pavlenko, T. Diluted Calcium Hydroxylapatite for Skin Tightening of the Upper Arms and Abdomen. *J. Drugs Dermatol.* **2017**, *16*, 900–906.
91. Nisbet, S.; Mahalingam, H.; Gfeller, C.F.; Biggs, E.; Lucas, S.; Thompson, M.; Cargill, M.R.; Moore, D.; Bielfeldt, S. Cosmetic benefit of a biomimetic lamellar cream formulation on barrier function or the appearance of fine lines and wrinkles in randomised proof-of-concept clinical studies. *Int. J. Cosmet. Sci.* **2018**. [CrossRef]
92. Yimam, M.; Lee, Y.C.; Jiao, P.; Hong, M.; Brownell, L.; Jia, Q. A Randomized, Active Comparator-controlled Clinical Trial of a Topical Botanical Cream for Skin Hydration, Elasticity, Firmness, and Cellulite. *J. Clin. Aesthet. Dermatol.* **2018**, *11*, 51–57.
93. Kanlayavattanakul, M.; Lourith, N.; Chaikul, P. Jasmine rice panicle: A safe and efficient natural ingredient for skin ageing treatments. *J. Ethnopharmacol.* **2016**, *193*, 607–616. [CrossRef]
94. Rodrigues, F.; Matias, R.; Ferreira, M.; Amaral, M.H.; Oliveira, M.B.P. In vitro and in vivo comparative study of cosmetic ingredients Coffee silverskin and hyaluronic acid. *Exp. Dermatol.* **2016**, *25*, 572–574. [CrossRef] [PubMed]
95. Bindra, R.M.; Imhof, R.E.; Mochan, A.; Eccleston, G.M. Opto-thermal technique for in-vivo stratum corneum hydration measurement. *Le J. Phys. IV* **1994**, *4*, C7-465–C7-468. [CrossRef]
96. Imhof, R.E.; Birch, D.J.S.; Thornley, F.R.; Gilchrist, J.R.; Strivens, T.A. Optothermal transient emission radiometry. *J. Phys. E Sci. Instrum.* **1984**, *17*, 521–525. [CrossRef]
97. Imhof, R.; Whitters, C.; Birch, D. Opto-thermal in-vivo monitoring of structural breakdown of an emulsion sunscreen on skin. *Clin. Mater.* **1990**, *5*, 271–278. [CrossRef]
98. Xiao, P. Photothermal Radiometry for Skin Research. *Cosmetics* **2016**, *3*, 10. [CrossRef]
99. Guo, X.; Imhof, R.E.; De Rigal, J. Spectroscopic Study of Water-Keratin Interactions in Stratum Corneum. *Anal. Sci.* **2001**, *17*, s342–s345.
100. Xiao, P.; Imhof, R.E. Optothermal skin-water concentration gradient measurement. *Proc. SPIE* **1996**, *2681*, 31–41. [CrossRef]
101. Xiao, P.; Packham, H.; Zheng, X.; Singh, H.; Elliott, C.; Berg, E.P.; Imhof, R.E. Opto-thermal radiometry and condenser-chamber method for stratum corneum water concentration measurements. *Appl. Phys. B* **2007**, *86*, 715–719. [CrossRef]

102. Xiao, P.; Wong, W.; Cottenden, A.M.; Imhof, R.E. In vivo stratum corneum over-hydration and water diffusion coefficient measurements using opto-thermal radiometry and TEWL Instruments. *Int. J. Cosmet. Sci.* **2012**, *34*, 328–331. [CrossRef]
103. Milner, T.E.; Smithies, D.J.; Goodman, D.M.; Lau, A.; Nelson, J.S. Depth determination of chromophores in human skin by pulsed photothermal radiometry. *Appl. Opt.* **1996**, *35*, 3379–3385. [CrossRef]
104. Choi, B.; Majaron, B.; Nelson, J.S. Computational model to evaluate port wine stain depth profiling using pulsed photothermal radiometry. *J. Biomed. Opt.* **2004**, *9*, 299–307. [CrossRef]
105. Jacques, S.L.; Nelson, J.S.; Wright, W.H.; Milner, T.E. Pulsed photothermal radiometry of port-wine-stain lesions. *Appl. Opt.* **1993**, *32*, 2439–2446. [CrossRef]
106. Xiao, P.; Ciortea, L.I.; Singh, H.; Berg, E.P.; Imhof, R.E. Opto-thermal radiometry for in-vivo nail measurements. *J. Phys. Conf. Ser.* **2010**, *214*, 012008. [CrossRef]
107. Xiao, P.; Ou, X.; Ciortea, L.I.; Berg, E.P.; Imhof, R.E. In Vivo Skin Solvent Penetration Measurements Using Opto-thermal Radiometry and Fingerprint Sensor. *Int. J. Thermophys.* **2012**, *33*, 1787–1794. [CrossRef]
108. Xiao, P.; Zheng, X.; Imhof, R.E.; Hirata, K.; McAuley, W.J.; Mateus, R.; Hadgraft, J.; Lane, M.E. Opto-Thermal Transient Emission Radiometry (OTTER) to image diffusion in nails in vivo. *Int. J. Pharm.* **2011**, *406*, 111–113. [CrossRef] [PubMed]
109. Vidovic, L.; Milanic, M.; Majaron, B. Objective characterization of bruise evolution using photothermal depth profiling and Monte Carlo modeling. *J. Biomed. Opt.* **2015**, *20*, 017001. [CrossRef] [PubMed]
110. Milanic, M.; Majaron, B. Spectral filtering in pulsed photothermal temperature profiling of collagen tissue phantoms. *J. Biomed. Opt.* **2009**, *14*, 064024. [CrossRef]
111. Majaron, B.; Milanic, M. Effective infrared absorption coefficient for photothermal radiometric measurements in biological tissues. *Phys. Med. Biol.* **2008**, *53*, 255–268. [CrossRef] [PubMed]
112. Leveque, J.L.; Escoubez, M.; Rasseneur, L. Water-keratin interaction in human stratum corneum. *Bioeng. Skin* **1887**, 227–242.
113. Bindra, R.M.; Imhof, R.E.; Eccleston, G.M. In-vivo opto-thermal measurement of epidermal thickness. *Le J. Phys. IV* **1994**, *04*, C7-445–C7-448. [CrossRef]
114. Cowen, J.A.; Imhof, R.E.; Xiao, P. Opto-thermal Measurement of Stratum Corneum Renewal Time. *Anal. Sci.* **2001**, *17*, s353–s356.
115. Notingher, I.; Imhof, R.E.; Xiao, P.; Pascut, F.C. Near-surface depth-resolved midinfrared emission spectroscopy. *Rev. Sci. Instrum.* **2003**, *74*, 346–348. [CrossRef]
116. Notingher, I.; Imhof, R.E.; Xiao, P.; Pascut, F.C. Spectral depth profiling of arbitrary surfaces by thermal emission decay-Fourier transform infrared spectroscopy. *Appl. Spectrosc.* **2003**, *57*, 1494–1501. [CrossRef]
117. Potts, R.O.; Guzek, D.B.; Harris, R.R.; McKie, J.E. A noninvasive, in vivo technique to quantitatively measure water concentration of the stratum corneum using attenuated total-reflectance infrared spectroscopy. *Arch. Dermatol. Res.* **1985**, *277*, 489–495. [CrossRef] [PubMed]
118. Bommannan, D.; Potts, R.; Guy, R. Examination of stratum corneum barrier function in vivo by infrared spectroscopy. *J. Investig. Dermatol.* **1990**, *95*, 403–408. [CrossRef]
119. Boncheva, M.; Damien, F.; Normand, V. Molecular organization of the lipid matrix in intact Stratum corneum using ATR-FTIR spectroscopy. *Biochim. Biophys. Acta* **2008**, *1778*, 1344–1355. [CrossRef]
120. Berthaud, F.; Boncheva, M. Correlation between the properties of the lipid matrix and the degrees of integrity and cohesion in healthy human Stratum corneum. *Exp. Dermatol.* **2011**, *20*, 255–262. [CrossRef]
121. Watkinson, A.; Lee, R.S.; Moore, A.E.; Pudney, P.D.A.; Paterson, S.E.; Rawlings, A.V. Reduced barrier efficiency in axillary stratum corneum. *Int. J. Cosmet. Sci.* **2002**, *24*, 151–161. [CrossRef]
122. Wang, C.; Zhu, J.; Zhang, D.; Yang, Y.; Zheng, L.; Qu, Y.; Yang, X.; Cui, X. Ionic liquid—microemulsions assisting in the transdermal delivery of Dencichine: Preparation, in-vitro and in-vivo evaluations, and investigation of the permeation mechanism. *Int. J. Pharm.* **2018**, *535*, 120–131. [CrossRef]
123. Binder, L.; Kulovits, E.M.; Petz, R.; Ruthofer, J.; Baurecht, D.; Klang, V.; Valenta, C. Penetration monitoring of drugs and additives by ATR-FTIR spectroscopy/tape stripping and confocal Raman spectroscopy—A comparative study. *Eur. J. Pharm. Biopharm.* **2018**, *130*, 214–223. [CrossRef] [PubMed]
124. Cilurzo, F.; Vistoli, G.; Selmin, F.; Gennari, C.G.M.; Musazzi, U.M.; Franzé, S.; Lo Monte, M.; Minghetti, P. An insight into the skin penetration enhancement mechanism of N-methylpyrrolidone. *Mol. Pharm.* **2014**, *11*, 1014–1021. [CrossRef] [PubMed]

125. Csizmazia, E.; Eros, G.; Berkesi, O.; Berko, S.; Szabo-Revesz, P.; Csanyi, E. Ibuprofen penetration enhance by sucrose ester examined by ATR-FTIR in vivo. *Pharm. Dev. Technol.* **2012**, *17*, 125–128. [CrossRef]
126. Obata, Y.; Utsumi, S.; Watanabe, H.; Suda, M.; Tokudome, Y.; Otsuka, M.; Takayama, K. Infrared spectroscopic study of lipid interaction in stratum corneum treated with transdermal absorption enhancers. *Int. J. Pharm.* **2010**, *389*, 18–23. [CrossRef] [PubMed]
127. Goh, C.F.; Craig, D.Q.M.; Hadgraft, J.; Lane, M.E. The application of ATR-FTIR spectroscopy and multivariate data analysis to study drug crystallisation in the stratum corneum. *Eur. J. Pharm. Biopharm.* **2017**, *111*, 16–25. [CrossRef]
128. Wolf, M.; Halper, M.; Pribyl, R.; Baurecht, D.; Valenta, C. Distribution of phospholipid based formulations in the skin investigated by combined ATR-FTIR and tape stripping experiments. *Int. J. Pharm.* **2017**, *519*, 198–205. [CrossRef]
129. Vyumvuhore, R.; Tfayli, A.; Manfait, M.; Baillet-Guffroy, A. Vibrational spectroscopy coupled to classical least square analysis, a new approach for determination of skin moisturizing agents' mechanisms. *Skin Res. Technol.* **2014**, *20*, 282–292. [CrossRef]
130. Caussin, J.; Rozema, E.; Gooris, G.S.; Wiechers, J.W.; Pavel, S.; Bouwstra, J.A. Hydrophilic and lipophilic moisturisers have similar penetration profiles but different effects on SC water distribution in vivo. *Exp. Dermatol.* **2009**, *18*, 954–961. [CrossRef] [PubMed]
131. Kilpatrick-Liverman, L.; Kazmi, P.; Wolff, E.; Polefka, T. The use of near-infrared spectroscopy in skin care applications. *Skin Res. Technol.* **2006**, *12*, 162–169. [CrossRef] [PubMed]
132. Hansen, J.R.; Yellin, W. NMR and Intrared Spectroscopic Studies of Stratum Corneum Hydration. In *Water Structure at the Water-Polymer Interface*; Jellinek, H.H.G., Ed.; Springer: Boston, MA, USA, 1972; pp. 19–28.
133. Gilard, V.; Martino, R.; Malet-Martino, M.; Riviere, M.; Gournay, A.; Navarro, R. Measurement of total water and bound water contents in human stratum corneum by in vitro proton nuclear magnetic resonance spectroscopy. *Int. J. Cosmet. Sci.* **1998**, *20*, 117–125. [CrossRef]
134. Yamamura, T.; Tezuka, T. The Water-Holding Capacity of the Stratum Corneum Measured by 1 H-NMR. *J. Investig. Dermatol.* **1989**, *93*, 160–164. [CrossRef] [PubMed]
135. Jokura, Y.; Ishikawa, S.; Tokuda, H.; Imokawa, G. Molecular Analysis of Elastic Properties of the Stratum Corneum by Solid-State 13C-Nuclear Magnetic Resonance Spectroscopy. *J. Investig. Dermatol.* **1995**, *104*, 806–812. [CrossRef]
136. Laule, C.; Tahir, S.; Chia, C.L.L.; Vavasour, I.M.; Kitson, N.; MacKay, A.L. A proton NMR study on the hydration of normal versus psoriatic stratum corneum: Linking distinguishable reservoirs to anatomical structures. *NMR Biomed.* **2010**, *23*, 1181–1190. [CrossRef] [PubMed]
137. Silva, C.L.; Topgaard, D.; Kocherbitov, V.; Sousa, J.J.S.; Pais, A.A.C.C.; Sparr, E. Stratum corneum hydration: Phase transformations and mobility in stratum corneum, extracted lipids and isolated corneocytes. *Biochim. Biophys. Acta* **2007**, *1768*, 2647–2659. [CrossRef] [PubMed]
138. Bjorklund, S.; Nowacka, A.; Bouwstra, J.A.; Sparr, E.; Topgaard, D. Characterization of Stratum Corneum Molecular Dynamics by Natural-Abundance 13C Solid-State NMR. *PLoS ONE* **2013**, *8*, e61889. [CrossRef] [PubMed]
139. Muta, K.; Inomata, S.; Fukuhara, T.; Nomura, J.; Nishiyama, T.; Tagawa, Y.I.; Amano, S. Inhibitory effect of the extract of rhizome of Curcuma longa L in gelatinase activity and its effect on human skin. *J. Biosci. Bioeng.* **2018**, *125*, 353–358. [CrossRef]
140. Tessema, E.N.; Gebre-Mariam, T.; Lange, S.; Dobner, B.; Neubert, R.H.H. Potential application of oat-derived ceramides in improving skin barrier function: Part 1. Isolation and structural characterization. *J. Chromatogr. B Anal. Technol. Biomed. Life Sci.* **2017**, *1065–1066*, 87–95. [CrossRef]
141. Hoppel, M.; Reznicek, G.; Kahlig, H.; Kotisch, H.; Resch, G.P.; Valenta, C. Topical delivery of acetyl hexapeptide-8 from different emulsions: Influence of emulsion composition and internal structure. *Eur. J. Pharm. Sci.* **2015**, *68*, 27–35. [CrossRef]
142. Pham, Q.D.; Topgaard, D.; Sparr, E. Tracking solvents in the skin through atomically resolved measurements of molecular mobility in intact stratum corneum. *Proc. Natl. Acad. Sci. USA* **2017**, *114*, E112–E121. [CrossRef]
143. Voegeli, D. The effect of washing and drying practices on skin barrier function. *J. Wound Ostomy Cont. Nurs.* **2008**, *35*, 84–90. [CrossRef]

144. Bittoun, J.; Saint-Jalmes, H.; Querleux, B.; Darrasse, L.; Jolivet, O.; Idy-Peretti, I.; Wartski, M.; Richard, S.; Leveque, J. In vivo high-resolution MR imageing of the skin in a whole-body system at 1.5 T. *Radiology* **1990**, *176*, 457–460. [CrossRef]
145. Richard, S.; Querleux, B.; Bittoun, J.; Idy-Peretti, I.; Jolivet, O.; Cermakova, E.; Lévêque, J. In vivo proton relaxation times analysis of the skin layers by magnetic resonance imageing. *J. Investig. Dermatol.* **1991**, *97*, 120–125. [CrossRef] [PubMed]
146. Franconi, F.; Akoka, S.; Guesnet, J.; Baret, J.; Dersigny, D.; Breda, B.; Muller, C.; Beau, P. Measurement of epidermal moisture content by magnetic resonance imageing: Assessment of a hydration cream. *Br. J. Dermatol.* **1995**, *132*, 913–917. [CrossRef] [PubMed]
147. Szayna, M.; Kuhn, W. In vivo and in vitro investigations of hydration effects of beauty care products by high-field MRI and NMR microscopy. *J. Eur. Acad. Dermatol. Venereol.* **1998**, *11*, 122–128. [CrossRef] [PubMed]
148. Mesrar, J.; Ognard, J.; Garetier, M.; Chechin, D.; Misery, L.; Ben Salem, D. In vivo skin moisturizing measurement by high-resolution 3 Tesla magnetic resonance imageing. *Skin Res. Technol.* **2017**, *23*, 289–294. [CrossRef] [PubMed]
149. Ablett, S.; Burdett, N.G.; Carpenter, T.A.; Hall, L.D.; Salter, D.C. Short echo time MRI enables visualisation of the natural state of human stratum corneum water in vivo. *Magn. Reson. Imageing* **1996**, *14*, 357–360. [CrossRef]
150. Mirrashed, F.; Sharp, J.C. In vivo quantitative analysis of the effect of hydration (immersion and Vaseline treatment) in skin layers using high-resolution MRI and magnetisation transfer contrast. *Skin Res. Technol.* **2004**, *10*, 14–22. [CrossRef]
151. Welzel, J.; Bruhns, M.; Wolff, H. Optical coherence tomography in contact dermatitis and psoriasis. *Arch. Dermatol. Res.* **2003**, *295*, 50–55. [CrossRef]
152. Mogensen, M.; Morsy, H.; Thrane, L.; Jemec, G. Morphology and epidermal thickness of normal skin imaged by optical coherence tomography. *Dermatology* **2008**, *217*, 14–20. [CrossRef]
153. Welzel, J.; Lankenau, E.; Birngruber, R.; Engelhardt, R. Optical coherence tomography of the human skin. *J. Am. Acad. Dermatol.* **1997**, *37*, 958–963. [CrossRef]
154. Mogensen, M.; Thrane, L.; Joergensen, T.; Andersen, P.; Jemec, G. Optical Coherence Tomography for Imageing of Skin and Skin Diseases. *Semin. Cutan. Med. Surg.* **2009**, *28*, 196–202. [CrossRef] [PubMed]
155. Tearney, G.; Brezinski, M.; Southern, J.; Bouma, B.; Hee, M.; Fujimoto, J. Determination of the refractive index of highly scattering human tissue by optical coherence tomography. *Opt. Lett.* **1995**, *20*, 2258–2260. [CrossRef]
156. Wilhelm, K.P.; Elsner, P.; Berardesca, E. *Bioengineering of the Skin: Skin Imageing and Analysis*; CRC Press: Boca Raton, FL, USA, 2006.
157. Knüttel, A.; Boehlau-Godau, M. Spatially confined and temporally resolved refractive index and scattering evaluation in human skin performed with optical coherence tomography. *J. Biomed. Opt.* **2000**, *5*, 83–93. [CrossRef]
158. Abuzahra, F.; Baron, J. Optical coherence tomography of the skin: A diagnostic light look. *Der Hautarzt; Zeitschrift für Dermatologie, Venerologie, und verwandte Gebiete* **2006**, *57*, 646. [CrossRef] [PubMed]
159. Xu, W.; Ranger-Moore, J.; Saboda, K.; Salasche, S.; Warneke, J.; Alberts, D. Investigating sun-damaged skin and actinic keratosis with optical coherence tomography: A pilot study. *Technol. Cancer Res. Treat.* **2003**, *2*, 525–535.
160. Gladkova, N.; Petrova, G.; Nikulin, N.; Radenska-Lopovok, S.; Snopova, L.; Chumakov, Y.; Nasonova, V.; Gelikonov, V.; Gelikonov, G.; Kuranov, R.; et al. In vivo optical coherence tomography imageing of human skin: Norm and pathology. *Skin Res. Technol.* **2000**, *6*, 6–16. [CrossRef] [PubMed]
161. Jensen, L.; Thrane, L.; Andersen, P.; Tycho, A.; Pedersen, F.; Andersson-Engels, S.; BendsU00D8e, N.; Svanberg, S.; Svanberg, K. Optical coherence tomography in clinical examination of non-pigmented skin malignancies. In Proceedings of the European Conference on Biomedical Optics, Munich, Germany, 22 June 2003.
162. Olmedo, J.; Warschaw, K.; Schmitt, J.; Swanson, D. Optical coherence tomography for the characterization of basal cell carcinoma in vivo: A pilot study. *J. Am. Acad. Dermatol.* **2006**, *55*, 408–412. [CrossRef] [PubMed]

163. Olmedo, J.; Warschaw, K.; Schmitt, J.; Swanson, D. Correlation of thickness of basal cell carcinoma by optical coherence tomography in vivo and routine histologic findings: A pilot study. *Dermatol. Surg.* **2007**, *33*, 421–426.
164. Strasswimmer, J.; Pierce, M.; Park, B. Characterization of basal cell carcinoma by multifunctional optical coherence tomography. *J. Investig. Dermatol.* **2003**, *121*, 0156.
165. Gambichler, T.; Orlikov, A.; Vasa, R.; Moussa, G.; Hoffmann, K.; Stucker, M.; Altmeyer, P.; Bechara, F. In vivo optical coherence tomography of basal cell carcinoma. *J. Dermatol. Sci.* **2007**, *45*, 167–173. [CrossRef]
166. Ulrich, M.; Stockfleth, E.; Roewert-Huber, J.; Astner, S. Noninvasive diagnostic tools for nonmelanoma skin cancer. *Br. J. Dermatol.* **2007**, *157*, 56–58. [CrossRef]
167. Sattler, E.; Kastle, R.; Welzel, J. Optical coherence tomography in dermatology. *J. Biomed. Opt.* **2013**, *18*, 061224. [CrossRef] [PubMed]
168. Schuh, S.; Kaestle, R.; Sattler, E.; Welzel, J. Comparison of different optical coherence tomography devices for diagnosis of non-melanoma skin cancer. *Skin Res. Technol.* **2016**, *22*, 395–405. [CrossRef]
169. Gambichler, T.; Moussa, G.; Sand, M.; Sand, D.; Orlikov, A.; Altmeyer, P.; Hoffmann, K. Correlation between clinical scoring of allergic patch test reactions and optical coherence tomography. *J. Biomed. Opt.* **2005**, *10*, 064030. [CrossRef] [PubMed]
170. Ropke, M.A.; Alonso, C.; Jung, S.; Norsgaard, H.; Richter, C.; Darvin, M.E.; Litman, T.; Vogt, A.; Lademann, J.; Blume-Peytavi, U.; et al. Effects of glucocorticoids on stratum corneum lipids and function in human skin-A detailed lipidomic analysis. *J. Dermatol. Sci.* **2017**, *88*, 330–338. [CrossRef] [PubMed]
171. Jung, S.; Lademann, J.; Darvin, M.E.; Richter, C.; Pedersen, C.B.; Richter, H.; Schanzer, S.; Kottner, J.; Blume-Peytavi, U.; Ropke, M.A. In vivo characterization of structural changes after topical application of glucocorticoids in healthy human skin. *J. Biomed. Opt.* **2017**, *22*, 76018. [CrossRef] [PubMed]
172. Crowther, J.; Sieg, A.; Blenkiron, P.; Marcott, C.; Matts, P.; Kaczvinsky, J.; Rawlings, A. Measuring the effects of topical moisturisers on changes in stratum corneum thickness, water gradients and hydration in vivo. *Br. J. Dermatol.* **2008**, *159*, 567–577. [CrossRef]
173. Trojahn, C.; Dobos, G.; Richter, C.; Blume-Peytavi, U.; Kottner, J. Measuring skin ageing using optical coherence tomography in vivo: A validation study. *J. Biomed. Opt.* **2015**, *20*, 045003. [CrossRef]
174. Florence, P.; Cornillon, C.; Darrasse, M.F.; Flament, F.; Panhard, S.; Diridollou, S.; Loussouarn, G. Functional and structural age-related changes in the scalp skin of Caucasian women. *Skin Res. Technol.* **2013**, *19*, 384–393. [CrossRef]
175. Mizuno, A.; Kitajima, H.; Kawauchi, K.; Muraishi, S.; Ozaki, Y. Near-infrared Fourier transform Raman spectroscopic study of human brain tissues and tumours. *J. Raman Spectrosc.* **1994**, *25*, 25–29. [CrossRef]
176. Frank, C.; McCreery, R.; Redd, D. Raman spectroscopy of normal and diseased human breast tissues. *Anal. Chem.* **1995**, *67*, 777–783. [CrossRef]
177. Alfano, R.; Liu, C.; Sha, W.; Zhu, H.; Akins, D.; Cleary, J.; Prudente, R.; Cellmer, E. Human breast tissues studied by IR Fourier transform Raman spectroscopy. *Lasers Life Sci.* **1991**, *4*, 23–28.
178. Feld, M.; Manoharan, R.; Salenius, J.; Orenstein-Carndona, J.; Roemer, T.; Brennan, J., III; Dasari, R.; Wang, Y. Detection and characterization of human tissue lesions with near-infrared Raman spectroscopy. *Proc. SPIE* **1995**, *2388*, 99.
179. Liu, C.; Das, B.; Glassman, W.; Tang, G.; Yoo, K.; Zhu, H.; Akins, D.; Lubicz, S.; Cleary, J.; Prudente, R.; et al. Raman, fluorescence, and time-resolved light scattering as optical diagnostic techniques to separate diseased and normal biomedical media. *J. Photochem. Photobiol. B Biol.* **1992**, *16*, 187–209. [CrossRef]
180. Mahadevan-Jansen, A.; Mitchell, M.; Ramanujamf, N.; Malpica, A.; Thomsen, S.; Utzinger, U.; Richards-Kortumt, R. Near-Infrared Raman Spectroscopy for In Vitro Detection of Cervical Precancers. *Photochem. Photobiol.* **1998**, *68*, 123–132. [CrossRef] [PubMed]
181. Gniadecka, M.; Wulf, H.; Nielsen, O.; Christensen, D.; Hercogova, J. Distinctive molecular abnormalities in benign and malignant skin lesions: Studies by Raman spectroscopy. *Photochem. Photobiol.* **1997**, *66*, 418–423. [CrossRef]
182. Stone, N.; Stavroulaki, P.; Kendall, C.; Birchall, M.; Barr, H. Raman spectroscopy for early detection of laryngeal malignancy: Preliminary results. *Laryngoscope* **2000**, *110*, 1756–1763. [CrossRef]
183. Duindam, H.; Vrensen, G.; Otto, C.; Puppels, G.; Greve, J. New approach to assess the cholesterol distribution in the eye lens: Confocal Raman microspectroscopy and filipin cytochemistry. *J. Lipid Res.* **1995**, *36*, 1139–1146.

184. Siebinga, I.; Vrensen, G.; De Mul, F.; Greve, J. Age-related changes in local water and protein content of human eye lenses measured by Raman microspectroscopy. *Exp. Eye Res.* **1991**, *53*, 233–239. [CrossRef]
185. Duindam, J.; Vrensen, G.; Otto, C.; Greve, J. Cholesterol, phospholipid, and protein changes in focal opacities in the human eye lens. *Investig. Ophthalmol. Vis. Sci.* **1998**, *39*, 94.
186. Romer, T.; Brennan, J.; Fitzmaurice, M.; Feldstein, M.; Deinum, G.; Myles, J.; Kramer, J.; Lees, R.; Feld, M. Histopathology of human coronary atherosclerosis by quantifying its chemical composition with Raman spectroscopy. *Circulation* **1998**, *97*, 878–885. [CrossRef]
187. Salenius, J.; Brennan, J.; Miller, A.; Wang, Y.; Aretz, T.; Sacks, B.; Dasari, R.; Feld, M. Biochemical composition of human peripheral arteries examined with nearinfrared Raman spectroscopy. *J. Vasc. Surg.* **1998**, *27*, 710–719. [CrossRef]
188. Barry, B.; Edwards, H.; Williams, A. Fourier transform Raman and infrared vibrational study of human skin: Assignment of spectral bands. *J. Raman Spectrosc.* **1992**, *23*, 641–645. [CrossRef]
189. Williams, A.; Edwards, H.; Barry, B. Raman spectra of human keratotic biopolymers: Skin, callus, hair and nail. *J. Raman Spectrosc.* **1994**, *25*, 95–98. [CrossRef]
190. Anigbogu, A.; Williams, A.; Barry, B.; Edwards, H. Fourier transform Raman spectroscopy of interactions between the penetration enhancer dimethyl sulfoxide and human stratum corneum. *Int. J. Pharm.* **1995**, *125*, 265–282. [CrossRef]
191. Lawson, E.; Anigbogu, A.; Williams, A.; Barry, B.; Edwards, H. Thermally induced molecular disorder in human stratum corneum lipids compared with a model phospholipid system; FT-Raman spectroscopy. *Spectrochim. Acta Part A Mol. Biomol. Spectrosc.* **1998**, *54*, 543–558. [CrossRef]
192. Caspers, P.; Williams, A.; Carter, E.; Edwards, H.; Barry, B.; Bruining, H.; Puppels, G. Monitoring the penetration enhancer dimethyl sulfoxide in human stratum corneum in vivo by confocal Raman spectroscopy. *Pharm. Res.* **2002**, *19*, 1577–1580. [CrossRef] [PubMed]
193. Caspers, P.; Lucassen, G.; Carter, E.; Bruining, H.; Puppels, G. In vivo confocal Raman microspectroscopy of the skin: Noninvasive determination of molecular concentration profiles. *J. Investig. Dermatol.* **2001**, *116*, 434–442. [CrossRef] [PubMed]
194. Caspers, P.; Lucassen, G.; Wolthuis, R.; Bruining, H.; Puppels, G. In vitro and in vivo Raman spectroscopy of human skin. *Biospectroscopy* **1998**, *4*, S31–S39. [CrossRef]
195. Caspers, P.; Lucassen, G.; Puppels, G. Combined in vivo confocal Raman spectroscopy and confocal microscopy of human skin. *Biophys. J.* **2003**, *85*, 572–580. [CrossRef]
196. Schallreuter, K.; Wood, J.; Farwell, D.; Moore, J.; Edwards, H. Oxybenzone oxidation following solar irradiation of skin: Photoprotection versus antioxidant inactivation. *J. Investig. Dermatol.* **1996**, *106*, 583–586. [CrossRef]
197. Gniadecka, M.; Nielsen, O.; Wessel, S.; Heidenheim, M.; Christensen, D.; Wulf, H. Water and protein structure in photoaged and chronically aged skin. *J. Investig. Dermatol.* **1998**, *111*, 1129–1132. [CrossRef] [PubMed]
198. Lee, M.; Won, K.; Kim, E.J.; Hwang, J.S.; Lee, H.K. Comparison of stratum corneum thickness between two proposed methods of calculation using Raman spectroscopic depth profiling of skin water content. *Skin Res. Technol.* **2018**, *24*, 504–508. [CrossRef]
199. Janssens, M.; van Smeden, J.; Puppels, G.J.; Lavrijsen, A.P.M.; Caspers, P.J.; Bouwstra, J.A. Lipid to protein ratio plays an important role in the skin barrier function in patients with atopic eczema. *Br. J. Dermatol.* **2014**, *170*, 1248–1255. [CrossRef] [PubMed]
200. Tfayli, A.; Jamal, D.; Vyumvuhore, R.; Manfait, M.; Baillet-Guffroy, A. Hydration effects on the barrier function of stratum corneum lipids: Raman analysis of ceramides 2, III and 5. *Analyst* **2013**, *138*, 6582–6588. [CrossRef] [PubMed]
201. Ogawa-Fuse, C.; Morisaki, N.; Shima, K.; Hotta, M.; Sugata, K.; Ichihashi, T.; Oguri, M.; Yoshida, O.; Fujimura, T. Impact of water exposure on skin barrier permeability and ultrastructure. *Contact Dermat.* **2018**. [CrossRef] [PubMed]
202. Biniek, K.; Tfayli, A.; Vyumvuhore, R.; Quatela, A.; Galliano, M.F.; Delalleau, A.; Baillet-Guffroy, A.; Dauskardt, R.H.; Duplan, H. Measurement of the biomechanical function and structure of ex vivo drying skin using raman spectral analysis and its modulation with emollient mixtures. *Exp. Dermatol.* **2018**, *27*, 901–908. [CrossRef]

203. Essendoubi, M.; Gobinet, C.; Reynaud, R.; Angiboust, J.F.; Manfait, M.; Piot, O. Human skin penetration of hyaluronic acid of different molecular weights as probed by Raman spectroscopy. *Skin Res. Technol.* **2016**, *22*, 55–62. [CrossRef]
204. Stettler, H.; Kurka, P.; Wagner, C.; Sznurkowska, K.; Czernicka, O.; Böhling, A.; Bielfeldt, S.; Wilhelm, K.P.; Lenz, H. A new topical panthenol-containing emollient: Skin-moisturizing effect following single and prolonged usage in healthy adults, and tolerability in healthy infants. *J. Dermatol. Treat.* **2017**, *28*, 251–257. [CrossRef]
205. Zeranska, J.; Pasikowska, M.; Szczepanik, B.; Mlosek, K.; Malinowska, S.; Debowska, R.M.; Eris, I. A study of the activity and effectiveness of recombinant fibroblast growth factor (Q40P/S47I/H93G rFGF-1) in anti-ageing treatment. *Postepy Dermatol. I Alergol.* **2016**, *33*, 28–36. [CrossRef]
206. Chrit, L.; Bastien, P.; Sockalingum, G.; Batisse, D.; Leroy, F.; Manfait, M.; Hadjur, C. An in vivo randomized study of human skin moisturization by a new confocal Raman fiber-optic microprobe: Assessment of a glycerol-based hydration cream. *Skin Pharmacol. Physiol.* **2006**, *19*, 207–215. [CrossRef] [PubMed]
207. Egawa, M.; Hirao, T.; Takahashi, M. In vivo estimation of stratum corneum thickness from water concentration profiles obtained with Raman spectroscopy. *Acta Dermato-Venereol.* **2007**, *87*, 4–8. [CrossRef]
208. Sieg, A.; Crowther, J.; Blenkiron, P.; Marcott, C.; Matts, P. Confocal Raman microspectroscopy: Measuring the effects of topical moisturisers on stratum corneum water gradient in vivo. *Proc. SPIE* **2006**, *6093*, 60930N.
209. Choe, C.; Schleusener, J.; Lademann, J.; Darvin, M.E. In vivo confocal Raman microscopic determination of depth profiles of the stratum corneum lipid organization influenced by application of various oils. *J. Dermatol. Sci.* **2017**, *87*, 183–191. [CrossRef] [PubMed]
210. Choe, C.; Lademann, J.; Darvin, M.E. Depth profiles of hydrogen bound water molecule types and their relation to lipid and protein interaction in the human stratum corneum in vivo. *Analyst* **2016**, *141*, 6329–6337. [CrossRef] [PubMed]
211. Eklouh-Molinier, C.; Gaydou, V.; Froigneux, E.; Barlier, P.; Couturaud, V.; Manfait, M.; Piot, O. In vivo confocal Raman microspectroscopy of the human skin: Highlighting of spectral markers associated to ageing via a research of correlation between Raman and biometric mechanical measurements. *Anal. Bioanal. Chem.* **2015**, *407*, 8363–8372. [CrossRef]
212. Boireau-Adamezyk, E.; Baillet-Guffroy, A.; Stamatas, G.N. Age-dependent changes in stratum corneum barrier function. *Skin Res. Technol.* **2014**, *20*, 409–415. [CrossRef]
213. Kikuchi, S.; Aosaki, T.; Bito, K.; Naito, S.; Katayama, Y. In vivo evaluation of lateral lipid chain packing in human stratum corneum. *Skin Res. Technol.* **2015**, *21*, 76–83. [CrossRef]
214. Quatela, A.; Miloudi, L.; Tfayli, A.; Baillet-Guffroy, A. In vivo Raman Microspectroscopy: Intra- and Intersubject Variability of Stratum Corneum Spectral Markers. *Skin Pharmacol. Physiol.* **2016**, *29*, 102–109. [CrossRef]
215. Richters, R.J.H.; Falcone, D.; Uzunbajakava, N.E.; Varghese, B.; Caspers, P.J.; Puppels, G.J.; van Erp, P.E.J.; van de Kerkhof, P.C.M. Sensitive Skin: Assessment of the Skin Barrier Using Confocal Raman Microspectroscopy. *Skin Pharmacol. Physiol.* **2017**, *30*, 1–12. [CrossRef]
216. Darlenski, R.; Fluhr, J.W. In vivo Raman Confocal Spectroscopy in the Investigation of the Skin Barrier. *Curr. Probl. Dermatol.* **2016**, *49*, 71–79. [CrossRef]
217. Tippavajhala, V.K.; Magrini, T.D.; Matsuo, D.C.; Silva, M.G.P.; Favero, P.P.; De Paula, L.R.; Martin, A.A. In Vivo Determination of moisturisers Efficacy on Human Skin Hydration by Confocal Raman Spectroscopy. *AAPS PharmSciTech* **2018**, *19*, 3177–3186. [CrossRef] [PubMed]
218. Souza, C.; Maia Campos, P.; Schanzer, S.; Albrecht, S.; Lohan, S.B.; Lademann, J.; Darvin, M.E.; Meinke, M.C. Radical-Scavenging Activity of a Sunscreen Enriched by Antioxidants Providing Protection in the Whole Solar Spectral Range. *Skin Pharmacol. Physiol.* **2017**, *30*, 81–89. [CrossRef] [PubMed]
219. Pudney, P.; Melot, M.; Caspers, P.; Van Der Pol, A.; Puppels, G. An In Vivo Confocal Raman Study of the Delivery of Trans Retinol to the Skin. *Appl. Spectrosc.* **2007**, *61*, 804–811. [CrossRef] [PubMed]
220. Egawa, M.; Sato, Y. In vivo evaluation of two forms of urea in the skin by Raman spectroscopy after application of urea-containing cream. *Skin Res. Technol.* **2015**, *21*, 259–264. [CrossRef]
221. Mélot, M.; Pudney, P.; Williamson, A.; Caspers, P.; Van Der Pol, A.; Puppels, G. Studying the effectiveness of penetration enhancers to deliver retinol through the stratum cornum by in vivo confocal Raman spectroscopy. *J. Control. Release* **2009**, *138*, 32–39. [CrossRef] [PubMed]

222. Weigmanna, J.; Barthelmesa, C.; Schaeferc, H.; Sterrya, G. Penetration of titanium dioxide microparticles in a sunscreen formulation into the horny layer and the follicular orifice. *Skin Pharmacol. Appl. Skin Physiol.* **1999**, *12*, 247–256.
223. Tfayli, A.; Piot, O.; Pitre, F.; Manfait, M. Follow-up of drug permeation through excised human skin with confocal Raman microspectroscopy. *Eur. Biophys. J.* **2007**, *36*, 104–1058. [CrossRef]
224. Song, Y.; Xiao, C.; Mendelsohn, R.; Zheng, T.; Strekowski, L.; Michniak, B. Investigation of iminosulfuranes as novel transdermal penetration enhancers: Enhancement activity and cytotoxicity. *Pharm. Res.* **2005**, *22*, 1918–1925. [CrossRef]
225. Ashtikar, M.; Langelüddecke, L.; Fahr, A.; Deckert, V. Tip-enhanced Raman scattering for tracking of invasomes in the stratum corneum. *Biochim. Biophys. Acta Gen. Subj.* **2017**, *1861*, 2630–2639. [CrossRef]
226. Lohan, S.B.; Saeidpour, S.; Solik, A.; Schanzer, S.; Richter, H.; Dong, P.; Darvin, M.E.; Bodmeier, R.; Patzelt, A.; Zoubari, G.; et al. Investigation of the cutaneous penetration behavior of dexamethasone loaded to nano-sized lipid particles by EPR spectroscopy, and confocal Raman and laser scanning microscopy. *Eur. J. Pharm. Biopharm.* **2017**, *116*, 102–110. [CrossRef] [PubMed]
227. Dos Santos, L.; Téllez S, C.A.; Sousa, M.P.J.; Azoia, N.G.; Cavaco-Paulo, A.M.; Martin, A.A.; Favero, P.P. In vivo confocal Raman spectroscopy and molecular dynamics analysis of penetration of retinyl acetate into stratum corneum. *Spectrochim. Acta Part A Mol. Biomol. Spectrosc.* **2017**, *174*, 279–285. [CrossRef] [PubMed]
228. Pot, L.M.; Coenraads, P.J.; Blomeke, B.; Puppels, G.J.; Caspers, P.J. Real-time detection of p-phenylenediamine penetration into human skin by in vivo Raman spectroscopy. *Contact Dermat.* **2016**, *74*, 152–158. [CrossRef] [PubMed]
229. Zhang, L.; Cambron, T.; Niu, Y.; Xu, Z.; Su, N.; Zheng, H.; Wei, K.; Ray, P. A MCR approach revealing protein, water and lipid depth profile in atopic dermatitis patients' stratum corneum via in vivo confocal Raman spectroscopy. *Anal. Chem.* **2019**. [CrossRef] [PubMed]
230. Perticaroli, S.; Yeomans, D.J.; Wireko, F.C.; Webber, J.T.; Werchowski, K.M.; Cambron, R.T.; Ray, P.J. Translating chemometric analysis into physiological insights from in vivo confocal Raman spectroscopy of the human stratum corneum. *Biochim. Biophys. Acta Biomembr.* **2019**, *1861*, 403–409. [CrossRef] [PubMed]
231. Martin, K. In vivo measurements of water in skin by near-infrared reflectance. *Appl. Spectrosc.* **1998**, *52*, 1001–1007. [CrossRef]
232. Martin, K. Direct measurement of moisture in skin by NIR spectroscopy. *J. Soc. Cosmet. Chem.* **1993**, *44*, 249–261.
233. Walling, P.; Dabney, J. Moisture in skin by near-infrared reflectance spectroscopy. *J. Soc. Cosmet. Chem.* **1989**, *40*, 151–171.
234. Arimoto, H.; Egawa, M. Non-contact skin moisture measurement based on near-infrared spectroscopy. *Appl. Spectrosc.* **2004**, *58*, 1439–1446. [CrossRef]
235. Arimoto, H.; Egawa, M. Skin moisture measurement based on near-infrared spectroscopy and regression analysis. In Proceedings of the 25th Annual International Conference of the IEEE Engineering in Medicine and Biology Society (IEEE Cat. No.03CH37439), Cancun, Mexico, 17–21 September 2003; Volume 4, pp. 3438–3441. [CrossRef]
236. Egawa, M.; Fukuhara, T.; Takahashi, M.; Ozaki, Y. Determining water content in human nails with a portable near-infrared spectrometer. *Appl. Spectrosc.* **2003**, *57*, 473–478. [CrossRef]
237. Egawa, M.; Arimoto, H.; Hirao, T.; Takahashi, M.; Ozaki, Y. Regional difference of water content in human skin studied by diffuse-reflectance near-infrared spectroscopy: Consideration of measurement depth. *Appl. Spectrosc.* **2006**, *60*, 24–28. [CrossRef]
238. McIntosh, L.M.; Jackson, M.; Mantsch, H.H.; Mansfield, J.R.; Crowson, A.N.; Toole, J.W.P. Near-infrared spectroscopy for dermatological applications. *Vib. Spectrosc.* **2002**, *28*, 53–58. [CrossRef]
239. Takiwaki, H.; Miyaoka, Y.; Arase, S. Analysis of the absorbance spectra of skin lesions as a helpful tool for detection of major pathophysiological changes. *Skin Res. Technol.* **2004**, *10*, 130–135. [CrossRef] [PubMed]
240. Atencio, J.A.D.; Rodriguez, M.C.; Montiel, S.V.y.; Gutierrez, J.L.; Martinez, F.; Gutierrez, B.; Orozco, E.; Castro, J.; Rodriguez, A.C. Diffuse Reflectance Spectroscopy of Human Skin Using a Commercial Fiber Optic Spectrometer. *AIP Conf. Proc.* **2008**, *1032*, 105–107. [CrossRef]
241. Dreassi, E.; Ceramelli, G.; Fabbri, L.; Vocioni, F.; Bartalini, P.; Corti, P. Application of Near-infrared Reflectance Spectrometry in the Studyof AtopyPart 1. Investigation of Skin Spectra. *Analyst* **1997**, *122*, 767–770. [CrossRef] [PubMed]

242. Dreassi, E.; Ceramelli, G.; Mura, P.; Perruccio, P.L.; Vocioni, F.; Bartalini, P.; Corti, P. Near-infrared Reflectance Spectrometry in the Studyof AtopyPart2. Interactions Between the Skin and Polyethylene Glycol400, Isopropyl Myristate and Hydrogel. *Analyst* **1997**, *122*, 771–776. [CrossRef]
243. Corti, P.; Ceramelli, G.; Dreassi, E.; Njine, M. Near infrared reflectance spectroscopy in the study of atopy Part 3.† Interactions between the skin and fomblins. *Analyst* **1998**, *123*, 2313–2317. [CrossRef]
244. Boden, I.; Nilsson, D.; Naredi, P.; Lindholm-Sethson, B. Characterization of healthy skin using near infrared spectroscopy and skin impedance. *Med. Biol. Eng. Comput.* **2008**, *46*, 985–995. [CrossRef]
245. Greve, T.M.; Kamp, S.; Jemec, G.B.E. Disease quantification in dermatology: In vivo near-infrared spectroscopy measures correlate strongly with the clinical assessment of psoriasis severity. *J. Biomed. Opt.* **2013**, *18*, 037006. [CrossRef]
246. De Rigal, J.; Losch, M.; Bazin, R.; Camus, C.; Sturelle, C.; Descamps, V.; Leveque, J. Near infrared spectroscopy: A new approach to the characterization of dry skin. *J. Soc. Cosmet. Chem.* **1993**, *44*, 197–209.
247. Egawa, M. In vivo simultaneous measurement of urea and water in the human stratum corneum by diffuse-reflectance near-infrared spectroscopy. *Skin Res. Technol.* **2009**, *15*, 195–199. [CrossRef] [PubMed]
248. Mohamad; M.; Msabbri, A.R.; MatJafri, M.Z. Conceptual design of near infrared spectroscopy instrumentation for skin moisture measurement. In Proceedings of the 2011 IEEE Colloquium on Humanities Science and Engineering, Penang, Malaysia, 5–6 December 2011; pp. 801–804. [CrossRef]
249. Wichrowski, K.; Sore, G.; Khaïat, A. Use of infrared spectroscopy for in vivo measurement of the stratum corneum moisturization after application of costmetic preparations. *Int. J. Cosmet. Sci.* **1995**, *17*, 1–11. [CrossRef] [PubMed]
250. Qassem, M.; Kyriacou, P. Use of reflectance near-infrared spectroscopy to investigate the effects of daily moisturiser application on skin optical response and barrier function. *J. Biomed. Opt.* **2014**, *19*. [CrossRef] [PubMed]
251. Qassem, M.; Kyriacou, P. In vivo investigation of short term skin water contact and moisturiser application using NIR Spectroscopy. In Proceedings of the 2013 35th Annual International Conference of the IEEE Engineering in Medicine and Biology Society (EMBC), Osaka, Japan, 3–7 July 2013.
252. Qassem, M.; Kyriacou, P.A. Reflectance near-infrared measurements for determining changes in skin barrier function and scattering in relation to moisturiser application. *J. Biomed. Opt.* **2015**, *20*, 095008. [CrossRef] [PubMed]
253. Qassem, M.; Kyriacou, P. Investigating skin barrier function utilizing reflectance NIR Spectroscopy. In Proceedings of the 2014 36th Annual International Conference of the IEEE Engineering in Medicine and Biology Society (EMBC), Chicago, IL, USA, 26–30 August 2014; pp. 3735–3738. [CrossRef]
254. Huang, X.; Yeo, W.H.; Liu, Y.; Rogers, J.A. Epidermal differential impedance sensor for conformal skin hydration monitoring. *Biointerphases* **2012**, *7*, 52. [CrossRef] [PubMed]
255. Webb, R.C.; Bonifas, A.P.; Behnaz, A.; Zhang, Y.; Yu, K.J.; Cheng, H.; Shi, M.; Bian, Z.; Liu, Z.; Kim, Y.S.; et al. Ultrathin conformal devices for precise and continuous thermal characterization of human skin. *Nat. Mater.* **2013**, *12*, 938–944. [CrossRef]
256. Krishnan, S.; Shi, Y.; Webb, R.C.; Ma, Y.; Bastien, P.; Crawford, K.E.; Wang, A.; Feng, X.; Manco, M.; Kurniawan, J.; et al. Multimodal epidermal devices for hydration monitoring. *Microsyst. Nanoeng.* **2017**, *3*, 17014. [CrossRef]
257. Woo, Y.; Ahn, J.; Chun, I.; Kim, H. Development of a method for the determination of human skin moisture using a portable near-infrared system. *Anal. Chem.* **2001**, *73*, 4964–4971. [CrossRef]

© 2019 by the authors. Licensee MDPI, Basel, Switzerland. This article is an open access article distributed under the terms and conditions of the Creative Commons Attribution (CC BY) license (http://creativecommons.org/licenses/by/4.0/).